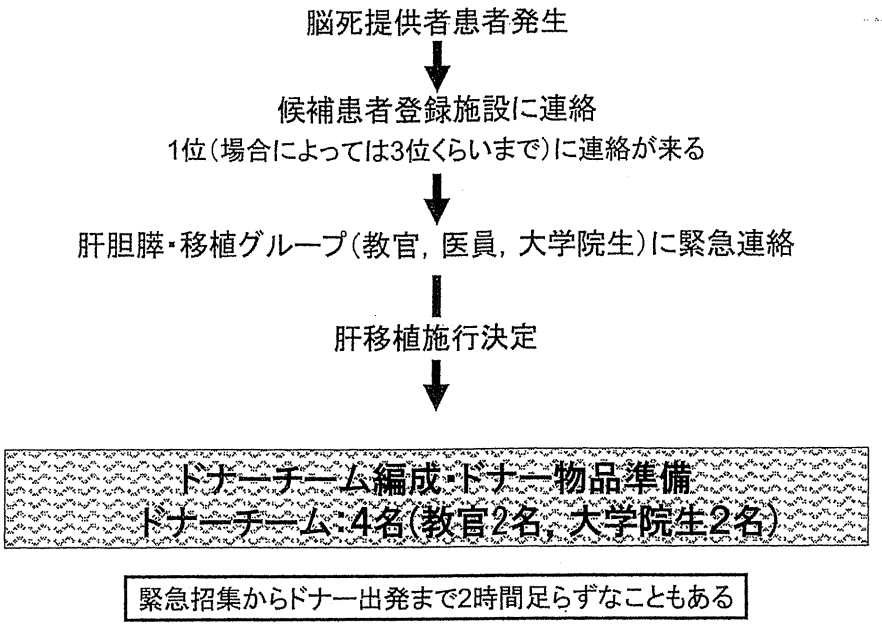

Figure 4. 臓器提供までの経過（大阪大学）.

とおりである．このことは，脳死肝移植医療が遅々として進行しなかった本邦では，何よりも喜ばしい事実である．また，脳死肝移植医療に対する関係各所の努力のたまものであることはいうまでもないし，進歩の1つである．

その一方で，最後にあげたいのは，移植施設側の問題である．現在，脳死肝移植認定施設は，全国に21施設（18歳未満限定の2施設を含む）ある（(社) 日本臓器移植ネットワーク http//www.jotnw.or.jp/index.html）．これらの施設は，現在肝移植のみを施行しているわけではない．というのは，当科同様，ほぼ全施設において肝移植以外に肝胆膵外科診療に従事している．筆者らの施設（大阪大学消化器外科）においても，肝移植医療に従事するのは，上部消化管，下部消化管配属をのぞく，肝胆膵・移植グループに所属する消化器外科医（教官6名と医員5名）である．他の脳死肝移植認定施設同様，通常は，日本肝胆膵外科学会高度技能医修練施設（日本肝胆膵外科学会 http://www.jshbps.jp/）として，肝臓外科，胆道外科，膵臓外科，生体肝移植など，年間約200例の手術を施行している．その中で，脳死提供者が発生するとFigure 4に示す時間経過でドナー摘出チームを招集し，提供施設に摘出に向かう．出発までの準備時間が，数時間のことも少なくない．また，ほとんどの症例において脳死臓器提供者発生の連絡は午前2～3時頃が多い．このため，人員の確保に難渋することもある．いずれにせよ，現在は本来研究に専念すべき大学院生の協力なしには，摘出チームの編成は困難である．また，Figure 5に示すように，約50kg以上の摘出手術関連物品を提供施設まで運搬する必要がある．その中には，保存液（UW 1L×6本）や保存液に入れる薬剤各種だけではなく，凍結生食（500ml×20パック）や冷却用氷（20kg）にくわえてスリッパ，マスク，帽子，手術用ガウン，手術用着，手袋，までが含まれる．このような状況が保険診療といえるのかどうか，これらの運搬に医師免許は必要なのかどうか，はなはだ疑問に感じているのは筆者らのみではないと思う．現在，教室では，これら器材・薬剤運搬も含めた緊急時の人員確保のために，2010年1月より，大阪市立大学と連携し，大阪大学附属病院・臨床登録医として摘出チームの一員として参加してもらっている．現在までに，2例の脳死肝移植実施症例において，摘出チームの人員不足においてご助力いただき，大変感謝している．今後，症例数の増加によっては，大阪府下の大阪医科大学，関西医科大学，近畿大学な

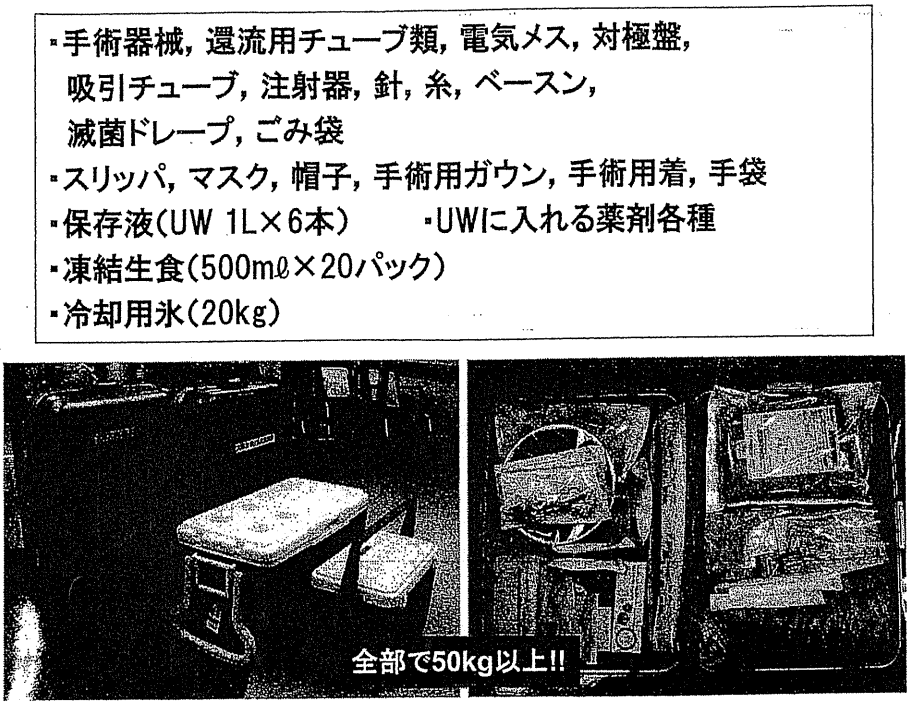

Figure 5. 肝提供者手術・準備物品．すべての準備物品は，大阪大学から提供施設へ医師4名で運ぶ．原則として，提供施設の物品は一切使用不可能．

ど他大学にもご協力をお願いし，脳死提供者摘出手術における，外科領域での診療連携を推進する必要性があるのではないかと考えている．

おわりに

近年，わが国の外科医療を取り巻く環境が大きく変化している．過剰労働や医療訴訟の増加などさまざまな要因により，外科志望者の減少が顕著となり，わが国の外科医数は1998年をピークに年々減少している．この外科医療崩壊の危機といっても過言ではない状況は脳死肝移植医療にも直結する．つまり，われわれがまさに直面している肝移植医療を志す外科医の激減である．このような状況への対策については，労働環境を改善することがその1つであることはいうまでもない[10]．特に脳死肝移植医療のように高度に複雑化された医療環境の中では，医療関係者それぞれの知識と専門性を生かした「チーム医療」が不可欠で，外科医の専門性を高め良好な就労環境で「肝移植医療」を展開することが最重要である．しかしながら，その現状にはほど遠く，提供者手術における50kgの器材・薬剤の運搬（Figure 5）はその象徴かもしれない．2007年4月日本外科学会は，第107回総会(会長：門田守人)において，今後の外科医療に対して，医療費，刑事司法，プロフェッショナリズムなどにくわえて，「医師に対する過重な負担を軽減するため，医師数の増加を図るとともに，コメディカルや医療事務等の充実により医師が本来業務に専念できるような体制を構築すべきである」との提言[11]を行った．脳死肝移植においても，移植外科医が減少し，その医療水準が維持できなくなるかもしれないという可能性がある今，移植医療のあるべき姿を考え，その構築に向けた取り組みを始めなければならない．改正臓器移植法案の施行が，表現は悪いかもしれないが，脳死肝移植を「お祭りから真の医療」に変える端緒になることを切に祈りたい．

本論文内容に関連する著者の利益相反
：永野浩昭（アステラス製薬株式会社）

文　献

1) 日本移植学会イスタンブール宣言アドホック翻訳委員会：臓器取引と移植ツーリズムに関するイスタンブール宣言．移植　43;368-377:2008

2) Exclusive Board WHO : Human organ and tissue transplantation. Agenda item 4.12, EB124. R13, 2009
3) 藤山みどり：宗教情報センター宗教情報（2010年9月25日），臓器移植法に賛成ですか？ 反対ですか？(http : //www.circam.jp/page.jsp?id=1364)
4) 玄田拓哉，市田隆文：我が国の肝移植ガイドラインを解釈する．肝・胆・膵 60 ; 293-302 : 2010
5) Raia S, Nery JR, Mies S : Liver transplantation from live donors. Lancet 2 ; 497 : 1989
6) Hashikura Y, Makuuchi M, Kawasaki S, et al : Successful living-related partial liver transplantation to an adult patient. Lancet 343 ; 1233-1234 : 1994
7) Surman OS : The ethics of partial-liver donation. N Engl J Med 346 ; 1038 : 2002
8) Wiesner R, Edwards E, Freeman R, et al : Model for end-stage liver disease (MELD) and allocation of donor livers. Gastroenterology 124 ; 91-96 : 2003
9) Kamath PS, Kim WR, Advanced Liver Disease Study Group : The model for end-stage liver disease (MELD). Hepatology 45 ; 797-805 : 2007
10) 西田 博，前原正明，富永隆治：チーム医療維新 一枚岩となって我が国の医療再生に必要な構造改革を！～米国チーム医療，NP・PAの現場を視察して～．日本外科学会雑誌 109 ; 299-306 : 2008
11) Monden M : Changing society, evolving surgery. Surg Today 38 ; 195-205 : 2008

〔論文受領，平成23年3月17日
受理，平成23年3月21日〕

AAC
Journals.ASM.org

Identification of Novel *N*-(Morpholine-4-Carbonyloxy) Amidine Compounds as Potent Inhibitors against Hepatitis C Virus Replication

Akiko Kusano-Kitazume,[a] Naoya Sakamoto,[a,b] Yukiko Okuno,[c] Yuko Sekine-Osajima,[a] Mina Nakagawa,[a,b] Sei Kakinuma,[a,b] Kei Kiyohashi,[a] Sayuri Nitta,[a] Miyako Murakawa,[a] Seishin Azuma,[a] Yuki Nishimura-Sakurai,[a] Masatoshi Hagiwara,[c] and Mamoru Watanabe[a]

Department of Gastroenterology and Hepatology[a] and Department for Hepatitis Control,[b] Tokyo Medical and Dental University, Tokyo, Japan, and Department of Anatomy and Developmental Biology, Graduate School of Medicine, Kyoto University, Kyoto, Japan[c]

To identify novel compounds that possess antiviral activity against hepatitis C virus (HCV), we screened a library of small molecules with various amounts of structural diversity using an HCV replicon-expressing cell line and performed additional validations using the HCV-JFH1 infectious-virus cell culture. Of 4,004 chemical compounds, we identified 4 novel compounds that suppressed HCV replication with 50% effective concentrations of ranging from 0.36 to 4.81 μM. *N'*-(Morpholine-4-carbonyloxy)-2-(naphthalen-1-yl) acetimidamide (MCNA) was the most potent and also produced a small synergistic effect when used in combination with alpha interferon. Structure-activity relationship (SAR) analyses revealed 4 derivative compounds with antiviral activity. Further SAR analyses revealed that the *N*-(morpholine-4-carbonyloxy) amidine moiety was a key structural element for antiviral activity. Treatment of cells with MCNA activated nuclear factor κB and downstream gene expression. In conclusion, *N*-(morpholine-4-carbonyloxy) amidine and other related morpholine compounds specifically suppressed HCV replication and may have potential as novel chemotherapeutic agents.

Hepatitis C virus (HCV) is a major human pathogen. It is associated with persistent liver infection, which leads to the development of chronic hepatitis, liver cirrhosis, and hepatocellular carcinoma (13). Treatment with pegylated interferon (IFN) and ribavirin is associated with significant side effects and is effective in only half the patients infected with HCV genotype 1 (6). More effective and more tolerable therapeutics are under development, and direct-acting antiviral agents (DAAs) for HCV infection are currently in advanced clinical trials. In combination with IFN and ribavirin, the HCV protease inhibitors telaprevir and boceprevir have recently been approved for treatment of genotype 1 HCV infection in the United States, Canada, Europe, and Asian countries (11, 12, 22). Although these two drugs can achieve higher sustained virologic response rates than IFN and ribavirin, their effects could be compromised by the emergence of highly prevalent drug-resistant mutants (25). Thus, it is crucial to use several different classes of DAAs in combination to improve efficacy and reduce viral breakthrough.

The HCV subgenomic replicon system has been widely used to screen compound libraries for inhibitors of viral replication, using reporter activity as a surrogate marker for HCV replication. We previously reported the successful adaptation of the Huh7/Rep-Feo replicon cell line to a high-throughput screening assay system (28). This approach contributed to the discovery of antiviral compounds, such as hydroxyl-methyl-glutaryl coenzyme A reductase inhibitors (10) and epoxide compounds (20). In our present study, we used the Huh7/Rep-Feo replicon cell line to screen a library of small molecules with various amounts of structural diversity to identify novel compounds possessing antiviral activity against HCV. We showed that the screening hit compounds inhibited HCV replication in an HCV genotype 2a (JFH-1) infectious-virus cell culture (29). The most potent compound was *N'*-(morpholine-4-carbonyloxy)-2-(naphthalen-1-yl) acetimidamide (MCNA). Structure-activity relationship (SAR) analyses revealed that the *N*-(morpholine-4-carbonyloxy) amidine moiety was a key structural element for antiviral activity. We also investigated the possible mechanisms of action of these compounds and showed that MCNA likely inhibited HCV replication through activation of the nuclear factor κB (NF-κB) pathway.

MATERIALS AND METHODS

Reagents and chemicals. Recombinant human alpha 2b interferon (IFN-α2b) was obtained from Schering-Plough (Kenilworth, NJ), the NS3/4A protease inhibitor BILN 2061 from Boehringer Ingelheim (Ingelheim, Germany), beta-mercaptoethanol from Wako (Osaka, Japan), and recombinant human tumor necrosis factor alpha (TNF-α) from Sigma (St. Louis, MO). The library of chemicals that were screened was provided by the Chemical Biology Screening Center at Tokyo Medical and Dental University. Information about the library is available at http://bsmdb.tmd.ac.jp. The important features of the library were the abundance of pharmacophores and the great diversity. Lipinski's rule of five was used to evaluate drug similarity (15). The purity of each chemical from the library was greater than 90%. For SAR analyses, 27 compounds were purchased from Assinex (Moscow, Russia), ChemBridge (San Diego, CA), ChemDiv (San Diego, CA), Enamine (Kiev, Ukraine), Maybridge (Cambridge, United Kingdom), Ramidus AB (Lund, Sweden), SALOR (St. Louis, MO), Scientific Exchange (Center Ossipee, NH), or Vitas-M (Moscow, Russia). The chemicals were all prepared at concentrations of 10 mM in dimethyl sulfoxide (Sigma) and stored at −20°C until they were used.

Cell lines and cell culture maintenance. Huh7 and Huh7.5.1 cell lines (32) were maintained in Dulbecco's modified Eagle's medium (Sigma)

Received 22 September 2011 Returned for modification 18 October 2011
Accepted 14 December 2011
Published ahead of print 27 December 2011
Address correspondence to Naoya Sakamoto, nsakamoto.gast@tmd.ac.jp.
A. Kusano-Kitazume and N. Sakamoto contributed equally to this work.
Supplemental material for this article may be found at http://aac.asm.org/.

doi:10.1128/AAC.05764-11

supplemented with 10% fetal bovine serum and incubated at 37°C under 5% CO_2. The maintenance medium for the HCV replicon-harboring cell line, Huh7/Rep-Feo, was supplemented with 500 μg/ml of G418 (Nacalai Tesque, Kyoto, Japan).

HCV replicon construction and cell culture. An HCV subgenomic replicon plasmid that contained Rep-Feo, pHC1bneo/delS (Rep-Feo-1b), was derived from the HCV-N strain. RNA was synthesized from pRep-Feo and transfected into Huh7 cells. After culture in the presence of G418, a cell line that stably expressed the replicon was established (28, 31).

Cell-based screening of antiviral activity. Huh7/Rep-Feo cells were seeded at a density of 4,000 cells/well in 100 μl of medium in 96-well plates and incubated for 24 h. Test compound solutions, 10 mM in 100% dimethyl sulfoxide (DMSO), were added to the wells; for primary screening, the final concentration was 5 μM. The assay plates were incubated as described above for another 48 h, and luciferase activity was measured with a luminometer (Perkin-Elmer) using the Bright-Glo Luciferase assay system (Promega) following the manufacturer's instructions. Assays were performed in triplicate, and the results were expressed as means and standard deviations (SD) as percentages of the controls. Compounds were considered hits if they inhibited >50% of the mean control luciferase activities. Compounds were considered cytotoxic if they reduced cell viability below 70% of the control in dimethylthiazol carboxymethoxyphenyl sulfophenyl tetrazolium (MTS) assays and were discarded. The hit compounds were then validated by secondary screening, which determined the antiviral activities of each compound serially diluted at concentrations ranging from 0.1 μM to 30 μM under Huh7/Rep-Feo cells cultured in an identical manner to the primary screen. Compounds inhibiting replication with a 50% effective concentration (EC_{50}) of <5 μM and a selectivity index (SI) of >5 were selected for further analysis.

MTS assay. To evaluate cell viability, MTS assays were performed using the CellTiter 96 Aqueous One Solution Cell Proliferation Assay (Promega) according to the manufacturer's directions.

Calculation of the EC_{50}, CC_{50}, and SI. The EC_{50} indicates the concentration of test compound that inhibits replicon-based luciferase activity by 50%. The 50% cytotoxic concentration (CC_{50}) indicates the concentration that inhibits cell viability by 50%. The EC_{50} and CC_{50} values were calculated using probit regression analysis (2, 26). The selectivity index was calculated by dividing the CC_{50} by the EC_{50}.

Reporter and expression plasmids. The plasmid pC1neo-Rluc-IRES-Fluc was constructed to analyze the HCV internal ribosome entry site (IRES)-mediated translation efficiency (19). The plasmid expressed a bicistronic mRNA containing the *Renilla* luciferase gene translated in a cap-dependent manner, and firefly luciferase was translated by HCV-IRES-mediated initiation. The plasmid pISRE-TA-Luc (Invitrogen, Carlsbad, CA) expressed the firefly luciferase reporter gene under the control of the interferon stimulation response element (ISRE). The plasmid pNF-κB-TA-Luc (Clontech Laboratories, Franklin Lakes, NJ) expressed the firefly luciferase reporter gene under the control of NF-κB. The plasmid pRL-CMV (Promega, Madison, WI), which expressed the *Renilla* luciferase gene under the control of the cytomegalovirus early promoter/enhancer, was used as a control for the transfection efficiency of pISRE-TA-Luc and pNF-κB-TA-Luc (8).

Western blot analysis. Fifteen micrograms of total cell lysates was separated using NuPage 4-to-12% Bis-Tris gels (Invitrogen) and blotted onto polyvinylidene difluoride membranes. Each membrane was incubated with primary antibodies followed by a peroxidase-labeled anti-IgG antibody and visualized by chemiluminescence reaction using the ECL Western Blotting Analysis System (Amersham Biosciences, Buckinghamshire, United Kingdom). The primary antibodies were anti-NS5A (BioDesign, Saco, ME), anti-HCV core (kindly provided by T. Wakita), anti-phospho-p65 (Ser536) (93H1; Cell Signaling Technology, Beverly, MA), anti-IκBα (Santa Cruz Biotechnology, Santa Cruz, CA), and anti-β-actin (Sigma) antibodies.

HCV-JFH1 virus cell culture. HCV-JFH1 RNA transcribed *in vitro* was transfected into Huh7.5.1 cells. The transfected cells were subcultured every 3 to 5 days. The culture supernatant was subsequently transferred onto Huh7.5.1 cells.

TABLE 1 Effects of the leading hit compounds on HCV replication[a]

Compound	EC_{50} (μM)	CC_{50} (μM)	SI
1	0.36 (0.22–0.58)	45.2 (35.9–56.9)	126
2	0.86 (0.73–1.02)	>100	>116
3	0.94 (0.76–1.06)	25.3 (19.8–32.3)	26.9
4	4.81 (3.79–6.12)	27.1 (17.1–58.0)	5.64

[a] The EC_{50} and CC_{50} values are reported, with 95% confidence intervals in parentheses, from a representative experiment performed in triplicate.

Real-time RT-PCR analysis. The protocols and primers for real-time RT-PCR analysis of HCV RNA have been described previously (17). Briefly, total cellular RNA was isolated using an RNeasy Minikit (Qiagen, Valencia, CA), reverse transcribed, and subjected to real-time RT-PCR analysis. Expression of mRNA was quantified using the TaqMan Universal PCR Master Mix (Applied Biosystems, Foster City, CA) and the ABI 7500 real-time PCR system (Applied Biosystems).

Analyses of drug synergism. The effects on HCV replication of antiviral hit compounds plus IFN-α or BILN 2061 were analyzed according to classical isobologram analyses (24, 28). Dose-inhibition curves for IFN or BILN 2061 and the test compounds were drawn, with the 2 drugs (IFN or BILN 2061 and each test compound) used alone or in combination. For each drug combination, the concentrations of IFN or BILN 2061 and test compound that inhibited HCV replication by 50% (EC_{50}s) were plotted against the fractional concentration of IFN or BILN 2061 and the compound on the *x* and *y* axes, respectively. A theoretical line of additivity was drawn between plots of the EC_{50}s obtained for either drug used alone. The combined effects of the 2 drugs were considered to be additive, synergistic, or antagonistic if the plots of the combined drugs were located on, below, or above the line of additivity, respectively.

Statistical analyses. Statistical analyses were performed using Welch's *t* test. *P* values of less than 0.01 were considered statistically significant.

RESULTS

Screening results. To identify novel regulators of HCV replication, 4,004 chemical compounds were screened using the Huh7/Rep-Feo replicon assay system. The primary screens identified 117 compounds that inhibited ≥50% of replicon luciferase activity at 5 μM. Of the 117 compounds, 74 were cytotoxic and could not be further evaluated. In the secondary screen, nontoxic primary hits were evaluated by determining the antiviral activities of serial dilutions at concentrations ranging from 0.1 μM to 30 μM. This screen identified 19 compounds with EC_{50}s of less than 5 μM and CC_{50} values 5-fold greater than the EC_{50} values. The effect of each secondary hit on HCV-NS5A protein expression was examined using Western blot analysis. Of the 19 compounds, 4 compounds, designated 1, 2, 3, and 4, suppressed HCV subgenomic replication, with EC_{50}s ranging from 0.36 to 4.81 μM and SIs ranging from 5.64 to more than 100 (Table 1 and Fig. 1A and B; see Table S1 in the supplemental material). By Western blot analysis, compounds 1, 2, and 3 decreased HCV-NS5A protein levels at concentrations of 5 μM after incubation for 48 h (Fig. 1C). Compared with compounds 1, 2, and 3, the effect of compound 4 on HCV-NS5A protein expression was not remarkable at a concentration of 5 μM, similar to the results from the luciferase assay shown in Fig. 1B. The effects of the compounds on the HCV replicon were further validated in the JFH-1 cell culture. As shown in Fig. 1D, compounds 1, 2, 3, and 4 significantly inhibited intracellular RNA replication of HCV-JFH1. Although compound 4 was negative by Western blot analysis, it decreased HCV replication in the other

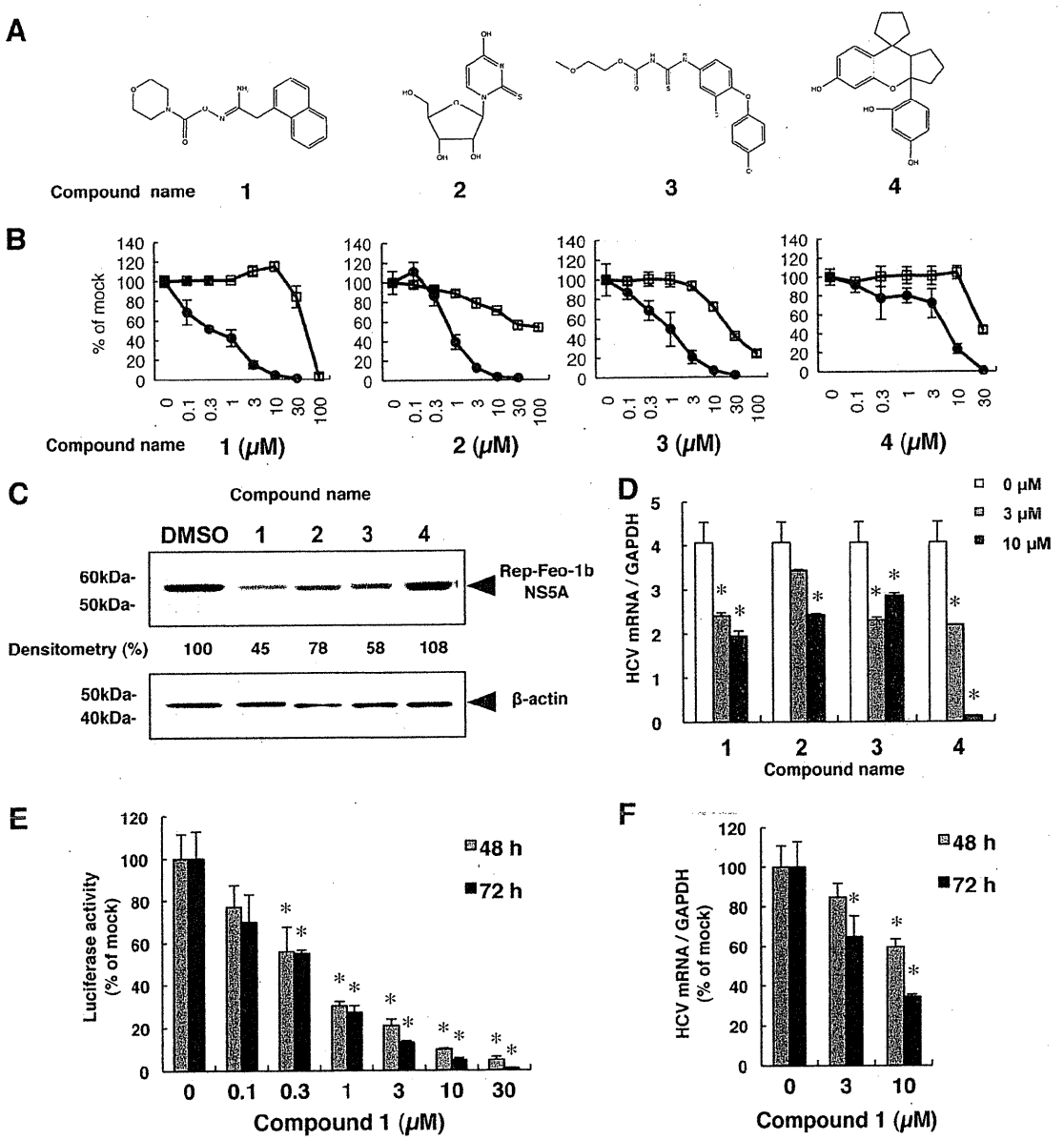

FIG 1 Effects of 4 screening hit compounds on HCV replication. (A) Chemical structures of hit compounds. (B) Huh7/Rep-Feo cells were treated with the indicated concentration of each compound for 48 h. Luciferase activities representing HCV replication are shown as percentages of the DMSO-treated control luciferase activity (solid circles). Cell viability is shown as a percentage of control viability (open squares). Each point represents the mean of triplicate data points, with the standard deviations represented as error bars. (C) Huh7/Rep-Feo cells were treated with DMSO or compounds 1 through 4 at 5 μM for 48 h, and Western blotting was performed using anti-HCV NS5A and anti-β-actin antibodies. Densitometry of NS5A protein was performed, and the results are indicated as percentages of the DMSO-treated control. The assay was repeated three times, and a representative result is shown. (D) Huh7.5.1 cells were transfected with HCV-JFH1 RNA and cultured in the presence of the indicated compounds at 3 μM or 10 μM. At 72 h after transfection, the cellular expression levels of HCV-RNA were quantified by real-time RT-PCR. The bars indicate means and SD. (E) Time-dependent reduction of luciferase activities in Huh7/Rep-Feo cells induced by compound 1. Luciferase activities are shown as percentages of the DMSO-treated control luciferase activity. The bars indicate means and SD. (F) Time-dependent reduction of cellular expression levels of HCV-RNA in HCV-JFH1-transfected cells induced by compound 1. HCV RNA levels are shown as percentages of the DMSO-treated control HCV-RNA level. The bars indicate means and SD. The asterisks indicate P values of less than 0.01.

assays, including the replicon and HCV-JFH1 virus assays. Thus, we concluded that compound 4 was an antiviral hit. These results indicated that the 4 compounds identified by cell-based screening suppressed subgenomic HCV replication and HCV replication in an HCV-based cell culture.

Hit compounds did not suppress HCV IRES-mediated translation. To determine whether the leading antiviral hits suppressed HCV IRES-dependent translation, we used the Huh7 cell line that had been stably transfected with pCIneo-Rluc IRES-Fluc. Treatment of these cells with the test compounds did not result in significant change in the internal luciferase activities at compound concentrations that suppressed expression of the HCV replicon (Fig. 2), suggesting that the effect of the hit compounds on HCV replication does not involve suppression of IRES-mediated viral-protein synthesis.

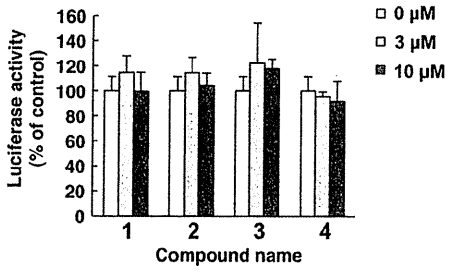

FIG 2 Hit compounds do not affect HCV IRES-mediated translation. The bicistronic reporter plasmid pC1neo-Rluc-IRES-Fluc was transfected into Huh7 cells. The cells were cultured in the presence of the indicated concentrations of compounds 1 through 4. After 6 h of treatment, luciferase activities were measured, and the values were normalized against *Renilla* luciferase activities. The assays were performed in triplicate. The bars indicate means and SD.

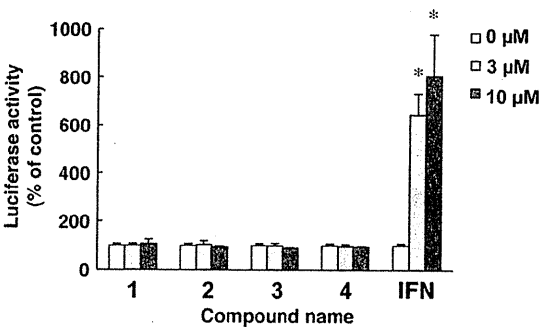

FIG 3 Hit compounds do not activate interferon-stimulated gene responses. Plasmids pISRE-TA-Luc and pRL-CMV were cotransfected into Huh7 cells. The transfected cells were cultured in the presence of the indicated concentrations of the hit compounds. After 6 h of treatment, luciferase activities were measured, and the values were normalized against *Renilla* luciferase activities. As positive controls, cells were treated with IFN-α at a concentration of 0, 3, or 10 U/ml. The bars indicate means and SD. The asterisks indicate *P* values of less than 0.01.

Hit compounds do not activate interferon-stimulated gene responses. To study whether the actions of the hit compounds involved IFN-mediated antiviral signaling that would induce expression of an IFN-stimulated gene, an ISRE-luciferase reporter plasmid, pISRE-TA-Luc, was transfected into Huh7 cells, and the transfected cells were cultured in the presence of the 4 compounds at concentrations of 0, 3, or 10 μM. In contrast to interferon, which elevated ISRE promoter activities significantly, the hit compounds showed no effects on the ISRE-luciferase activities (Fig. 3). These results indicated that the action of the hit compounds is independent of interferon signaling.

Drug synergism with IFN-α or BILN 2061. To investigate whether the hit compounds were synergistic with IFN-α or the protease inhibitor BILN 2061, we used isobologram analyses (24, 28). HCV replicon cells were treated with a combination of IFN-α or BILN 2061 and each hit compound at an EC_{50} ratio of 1:0. 4:1, 3:2, 2:3, 1:4, or 0:1, and the dose-effect results were plotted (Fig. 4A and C). The fractional EC_{50}s for IFN-α or BILN 2061 and each compound were plotted on the *x* and *y* axes, respectively, to generate an isobologram. As shown in Fig. 4B, all plots of the fractional EC_{50}s of compound 1 and IFN-α fell below the line of additivity, while the plots were located closed to the line of additivity for the treatments using IFN-α plus compound 2 or 3 and above the line for the treatment using IFN-α plus compound 4. Those results indicated that the anti-HCV effect of compound 1 was synergistic with IFN-α, the anti-HCV effects of compounds 2 and 3 were additive, and the effect of compound 4 was antagonistic. In the BILN 2061 combination study, the combination with compound 2 was slightly synergistic, while the combination with compound 1 or 3 was additive, and the combination with compound 4 was antagonistic (Fig. 4D).

SARs of compound 1 and similar compounds. We next conducted SAR analyses for hit compound 1 by screening 69 compounds with structures similar to that of compound 1 (see Table S2 in the supplemental material). Out of those compounds, we identified 4 structural analogues that suppressed subgenomic HCV replication with EC_{50}s ranging from 1.82 to 4.03 μM and SIs of 6.01 through >43.7 (Table 2 and Fig. 5A and B). Similarly, the 4 compounds designated 5, 6, 7, and 8 substantially decreased HCV-NS5A protein expression levels following treatment with the compounds (Fig. 5C). Consistent with the replicon results, the compounds significantly suppressed HCV-JFH1 mRNA in cell culture (Fig. 5D). Although the suppressive activities of the 4 compounds were similar, the original compound 1 showed the greatest anti-HCV activity. Therefore, we conducted SAR analyses of the compound 1 *N*-(morpholine-4-carbonyloxy) amidine and *N*-acyloxy-1-naphthalenacetamidine moieties. We screened 13 compounds containing *N*-(morpholine-4-carbonyloxy) amidine and 11 with *N*-acyloxy-1-naphthalenacetamidine (Fig. 6A; see Table S3 in the supplemental material). Intriguingly, 11 out of the 13 *N*-(morpholine-4-carbonyloxy) amidine compounds suppressed the subgenomic HCV replicon without cytotoxicity at a fixed concentration of 5 μM. In contrast, only 2 *N*-acyloxy-1-naphthalenacetamidine compounds decreased HCV replication (Fig. 6B and C). We also conducted dose-dependent suppression assays for HCV replicon. As shown in Table 3, 11 out of 13 *N*-(morpholine-4-carbonyloxy) amidine compounds consistently decreased subgenomic HCV replication, with EC_{50}s ranging from 1.52 through 8.62 μM and SIs of 14.2 to >61.4. Of these 11 compounds, compound 14 was the most potent, with an EC_{50} of 1.63 μM and an SI of >61.4. The antiviral effect of compound 14 against HCV-JFH1 was identical to that of the original compound 1. To identify the moiety conferring anti-HCV activity, we tested the morpholine-4-carboxyl moiety within the *N*-(morpholine-4-carboynloxy) amidine structure (Fig. 6D). Three compounds bearing the morpholine-4-carboxyl moiety were tested, and none showed suppressive activity toward the HCV replicon. These results suggested that the entire *N*-(morpholine-4-carbonyloxy) amidine moiety was important for efficient anti-HCV activity.

Effect of compound 1 on the NF-κB signaling pathway. NF-κB, composed of homo- and heterodimeric complexes of Rel-like domain-containing proteins, including p50 and p65, is a key regulator of innate and adaptive immune responses through transcriptional activation of several antiviral proteins (9, 23). We performed luciferase reporter assays, a p65 phosphorylation assay, and an IκB-α degradation assay to assess the effect of compound 1 on NF-κB signaling in host cells. Intriguingly, treatment of both Huh7 cells and HCV replicon-expressing cells with compound 1 increased NF-κB reporter activity in a dose-dependent manner (Fig. 7A and B). Consistently, treatment with compound 1 increased phosphorylated NF-κB p65 in Huh7 cells (Fig. 7C). Acti-

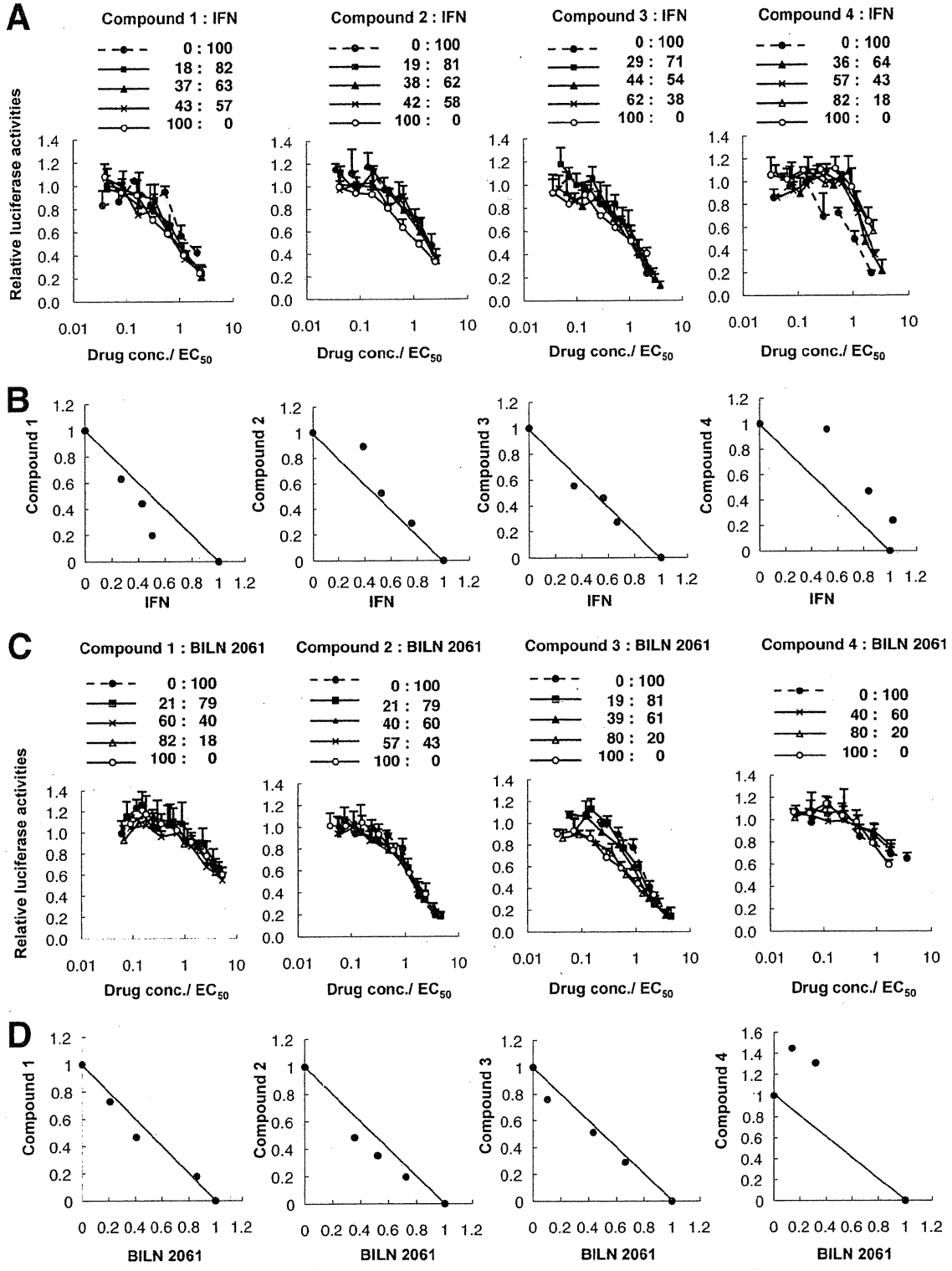

FIG 4 Drug synergism analyses: effects of each of the 4 antiviral hit compounds combined with IFN-α or BILN 2061 on HCV replication. (A and C) Huh7/Rep-Feo cells were cultured with a combination of IFN-α or BILN 2061 and antiviral hit compound 1, 2, 3, or 4 at the indicated ratios, adjusted by the EC_{50} of the individual drug. The internal luciferase activities were measured after 48 h of culture. Assays were performed in triplicate. Shown are means and SD. (B and D) Graphical presentations of isobologram analyses. For each drug combination in panels A and C, the EC_{50}s of IFN-α or BILN 2061 and compound 1, 2, 3, or 4 for inhibition of HCV replication were plotted against the fractional concentrations of IFN-α or BILN 2061 and each compound, as indicated on the x and y axis, respectively. A theoretical line of additivity is drawn between the EC_{50}s for each drug alone.

TABLE 2 Effects of derivative compounds of 1 on HCV replication[a]

Compound	EC_{50} (μM)	CC_{50} (μM)	SI
5	1.82 (0.58–5.68)	45.1 (14.3–52.5)	24.8
6	2.29 (1.57–3.34)	>100	>43.7
7	2.83 (1.43–5.78)	17.0 (5.25–38.7)	6.01
8	4.03 (3.51–4.63)	87.8 (59.1–172)	21.8

[a] The EC_{50} and CC_{50} values are reported, with 95% confidence intervals in parentheses, from a representative experiment performed in triplicate.

vation of NF-κB involves degradation of a suppressor protein, IκB-α. As shown in Fig. 7D, IκB-α protein levels were strongly decreased in cells treated with compound 1. Additionally, activation of the NF-κB pathway by TNF-α treatment significantly suppressed HCV replication (Fig. 7E). These results indicated that the antiviral action of compound 1 partially involved activation of the NF-κB signaling pathway.

DISCUSSION

Using a chimeric luciferase reporter-based subgenomic HCV-Feo replicon assay and an HCV-JFH1 cell culture, we discovered 4 novel anti-HCV compounds from cell-based screening of a library of 4,004 chemicals (Fig. 1 and Table 1). These compounds displayed anti-HCV activity at noncytotoxic concentrations. The most potent of the leading hit compounds was MCNA, and SAR analyses revealed that 4 compounds with structures similar to that of MCNA also had antiviral activity (Fig. 5). Furthermore, we showed that the *N*-(morpholine-4-carbonyloxy) amidine moiety within the structure of MCNA is essential for antiviral activity (Fig. 6).

After the development of the HCV replicon system, the study of HCV replication and discovery of novel anti-HCV agents have shown great progress. To date, our group and others have already made several successful attempts to discover novel inhibitors of HCV replication. Using Huh7/Rep-Feo cells, we previously identified novel anti-HCV substances, including cyclosporins (18, 19), short interfering RNA (siRNA) (31), hydroxyl-methyl-glutaryl coenzyme A reductase inhibitors (10), and epoxide compounds (20). Huh7/Rep-Feo cells were also used for screening a whole-genome siRNA library and successfully identified human genes that support HCV replication (27). Although the HCV replicon system cannot screen for inhibitors of viral entry and release, it is still a useful tool for rapid, reliable, and reproducible high-throughput screening. In our study, we used library sets of compounds that had probably not been used for anti-HCV drug screening before.

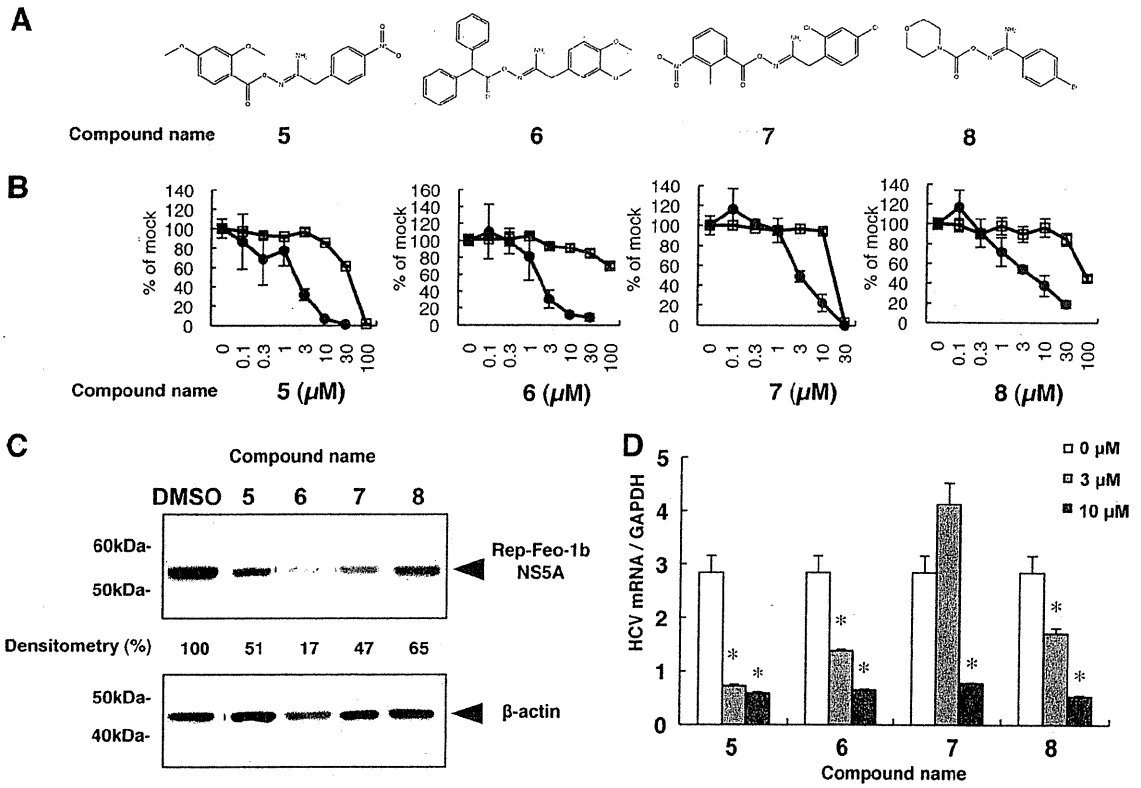

FIG 5 Effects of derivatives of compound 1 on HCV replication. (A) Chemical structures of screening hits of compound 1 derivatives. (B) Huh7/Rep-Feo cells were treated with various concentrations of each compound for 48 h. Luciferase activity for HCV RNA replication is shown as a percentage of the DMSO-treated control luciferase activity (solid circles). Cell viability is also shown as a percentage of control viability (open squares). Each point represents the mean of triplicate data points, with standard deviations represented as error bars. (C) HCV NS5A protein expression levels in Huh7/Rep-Feo cells after treatment with the hit compounds. Huh7/Rep-Feo cells were treated with DMSO and derivative compounds at 5 μM for 48 h, and Western blotting was performed using anti-HCV NS5A and anti-β-actin antibodies. Densitometry of the NS5A protein was performed, and the results are indicated as percentages of the DMSO-treated control. The assay was repeated three times, and a representative result is shown. (D) Huh7.5.1 cells were transfected with HCV-JFH1 RNA and cultured in the presence of the indicated compounds at a concentration of 3 μM or 10 μM. At 72 h after transfection, total cellular RNA was extracted, followed by real-time RT-PCR. The bars indicate means and SD. The asterisks indicate *P* values of less than 0.01. GAPDH, glyceraldehyde-3-phosphate dehydrogenase.

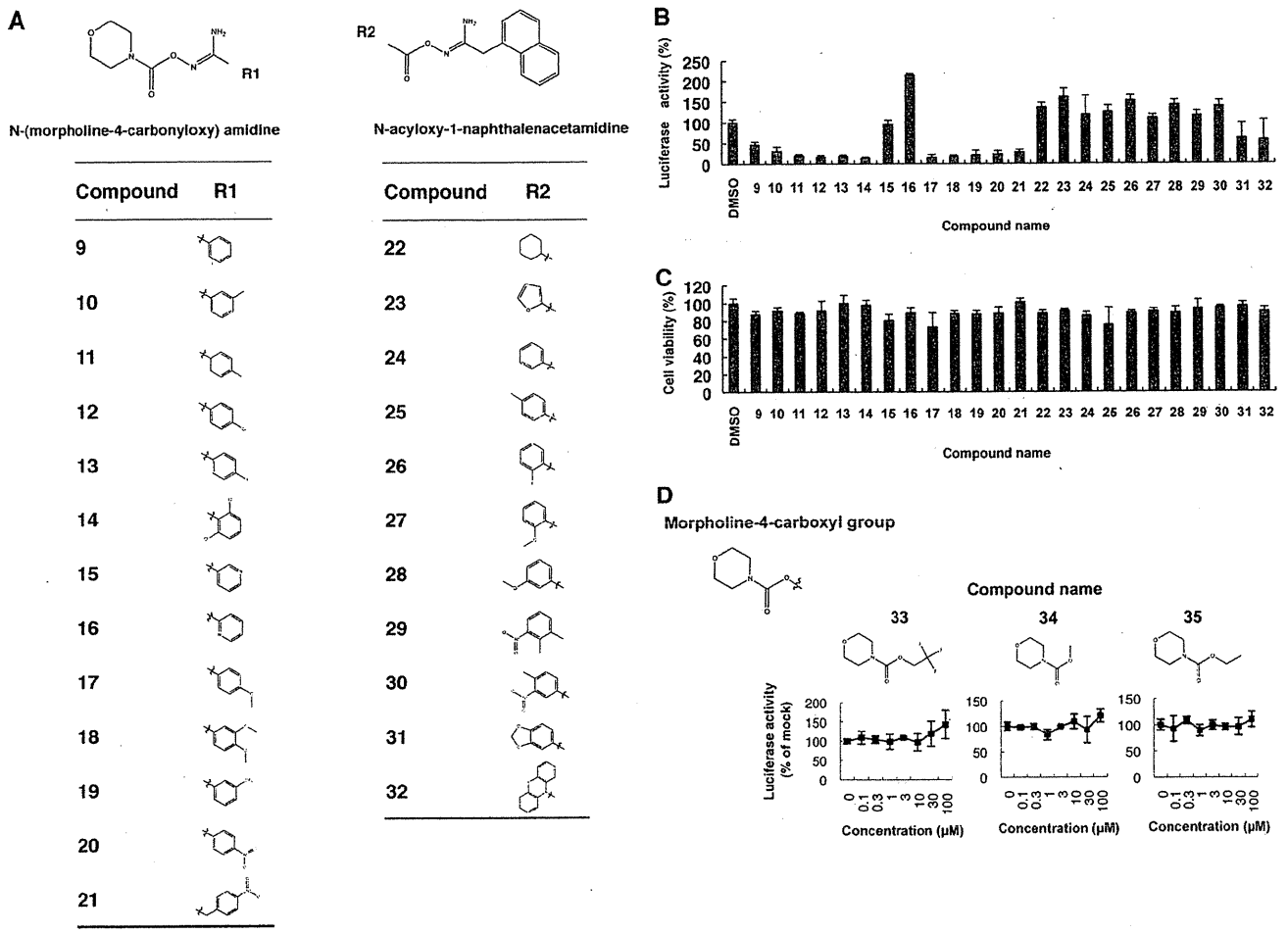

FIG 6 SARs of derivatives of compound 1 that contain *N*-(morpholine-4-carbonyloxy) amidine or *N*-acyloxy-1-naphthalenacetamidine moieties. (A) Chemical structures of compounds with *N*-(morpholine-4-carbonyloxy) amidine or *N*-acyloxy-1-naphthalenacetamidine analyzed for SARs. (B) Huh7/Rep-Feo cells were cultured in the presence of 13 compounds with *N*-(morpholine-4-carbonyloxy) amidine and 11 compounds with *N*-acyloxy-1-naphthalenacetamidine at a fixed concentration of 5 μM. The internal luciferase activities were measured after 48 h of culture. Luciferase activity for HCV RNA replication levels is shown as a percentage of the drug-negative (DMSO) control. Assays were performed in triplicate. The bars indicate means and SDs. (C) Cell viability is shown as a percentage of control viability. Assays were performed in triplicate. The bars indicate means and SD. (D) Effects of morpholine-4-carboxyl compounds on HCV replication. Huh7/Rep-Feo cells were treated with various concentrations of compound 33, 34, or 35 for 48 h. Luciferase activity for HCV RNA replication levels is shown as a percentage of the drug-negative (DMSO) control. Each point represents the mean of triplicate data points, with standard deviations represented as error bars.

TABLE 3 Effects of *N*-(morpholine-4-carbonyloxy) amidine compounds on HCV replication[a]

Compound	EC_{50} (μM)	CC_{50} (μM)	SI
9	8.62 (7.03–10.6)	>100	>11.1
10	3.32 (2.28–4.84)	47.0 (15.7–76.4)	14.2
11	1.55 (1.04–2.30)	48.8 (12.8–95.6)	31.5
12	1.52 (1.14–2.02)	51.0 (16.2–96.7)	33.6
13	1.60 (1.36–1.88)	38.6 (29.4–50.7)	24.1
14	1.63 (1.34–2.00)	>100	>61.4
15	ND	ND	ND
16	ND	ND	ND
17	1.77 (1.39–2.26)	63.3 (21.8–128)	35.8
18	3.80 (2.48–5.83)	100 (86.8–138)	26.3
19	1.99 (1.59–2.48)	55.1 (14.8–105)	27.7
20	2.61 (1.68–4.05)	>100	>38.3
21	1.55 (1.45–1.67)	94.6 (93.0–98.0)	61.0

[a] The EC_{50} and CC_{50} values are reported, with 95% confidence intervals in parentheses, from a representative experiment performed in triplicate. ND, not determined.

The morpholine moiety is a common pharmacophore present in many biosynthetic compounds, such as antimycotic agents (4, 21), and inhibitors of phosphoinositide 3-kinases (5, 16, 30), TNF-α-converting enzymes (14), and matrix metalloproteinases (1). Among the antimycotic morpholine derivatives, amorolfine has been widely used to treat onychomycosis (4, 21). The morpholino oxygen in a synthetic phosphoinositide 3-kinase inhibitor, LY294002, participated directly in a key hydrogen-bonding interaction at the ATP-binding site of phosphoinositide 3-kinase γ (30). Although the morpholine moieties are key components of many inhibitors, anti-HCV morpholine compounds have not yet been reported. In this report, we demonstrated for the first time that a morpholine-bearing compound, *N*-(morpholine-4-carbonyloxy) amidine, had a potent antiviral effect on HCV replication.

Among the 4 hit compounds, MCNA activated the NF-κB pathway (Fig. 7A, B, C, and D). NF-κB is a central regulator of innate and adaptive immune responses. NF-κB-induced tran-

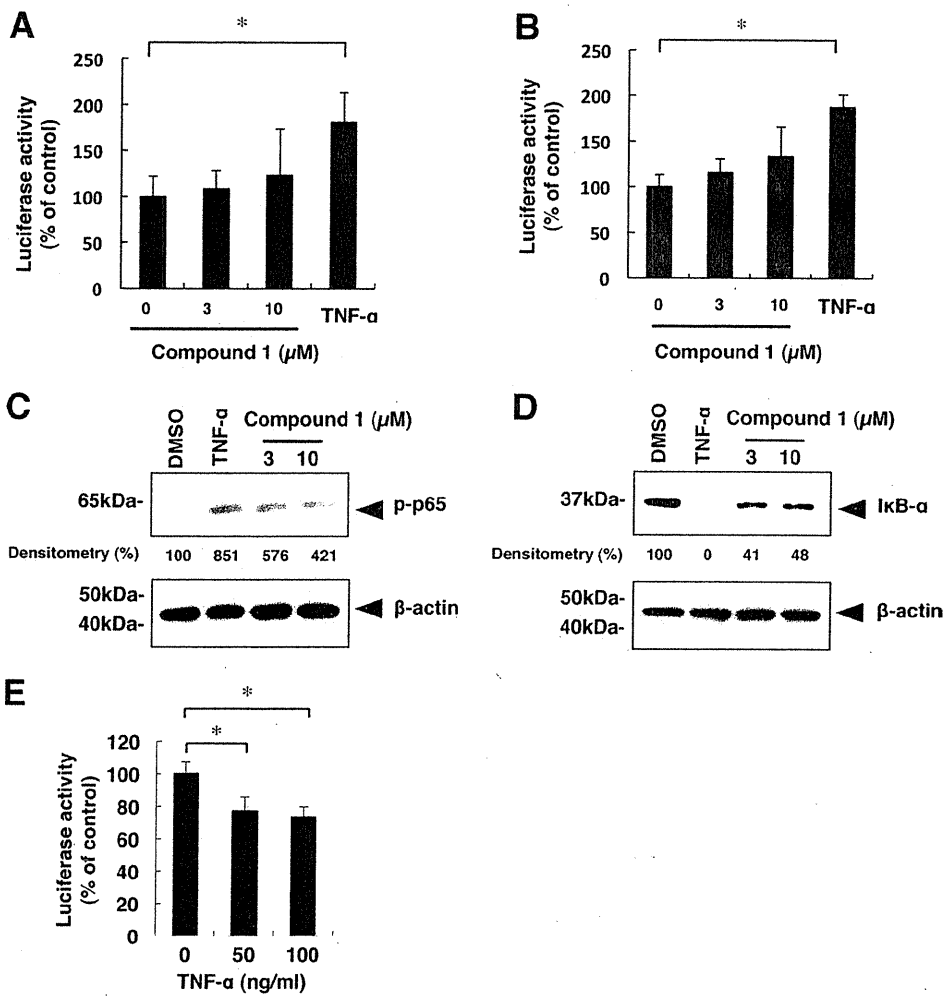

FIG 7 Effects of compound 1 on the NF-κB signaling pathway. (A and B) NF-κB-responsive luciferase reporter assays. The plasmids pNF-κB-TA-Fluc and pRL-CMV were cotransfected into Huh7 cells (A) or HCV replicon-expressing cells (B). At 24 h after transfection, cells were treated with compound 1 at a concentration of 0, 3, or 10 μM. After 6 h, luciferase activities were measured, and the values were normalized against *Renilla* luciferase activities. As a positive control, cells were treated with TNF-α (50 ng/ml). Assays were performed in triplicate. The bars indicate means and SD. (C and D) Huh7 cells were treated for 30 min with compound 1 at concentrations of 3 and 10 μM, and Western blot analyses of phosphorylated p65 and IκBα were conducted. As a positive control, cells were treated with TNF-α (50 ng/ml). β-Actin served as a loading control. Densitometry of phosphorylated p65 protein and IκB-α protein was performed, and the results are indicated as percentages of the DMSO-treated control. The assay was repeated three times, and a representative result is shown. (E) Effect of activation of NF-κB signaling on HCV RNA replication. Huh7/Rep-Feo cells were treated with TNF-α at a concentration of 0, 50, or 100 ng/ml for 48 h. Luciferase activity for HCV RNA replication levels is shown as a percentage of untreated negative-control luciferase activity. Assays were performed in replicates of 6. The asterisks indicate *P* values of less than 0.01.

scription is induced in response to a variety of signals, including proinflammatory cytokines, stress induction, and by-products of microbial and viral infection (9). In HCV-infected cells, activation of transcription factors, such as NF-κB and many interferon regulatory factors, proceeds mainly through Toll-like receptors and RIG-I-dependent host signaling pathways triggered by double-stranded RNA products (3). NF-κB, interferon regulatory factor 1, and interferon regulatory factor 3 bind to the positive regulatory domains of the IFN-β promoter to induce IFN-β expression and elicit antiviral states in host cells (23). Therefore, we hypothesized that the augmentation of host antiviral response through NF-κB activation is an important strategy for anti-HCV treatment. Our demonstration that the activation of NF-κB signaling suppressed HCV replication appears to follow this strategy (Fig. 7E). In support of the idea, Toll-like receptor 7 agonist has shown anti-HCV effects in a preclinical study (7). The anti-HCV activities of MCNA cannot be explained solely by NF-κB activation, because its antiviral activity was much more potent than selective NF-κB activation by TNF-α treatment (Fig. 7E). There remains the possibility that MCNA has a direct viral target. It will be important to assess whether long-term exposure to the compounds could select resistant variants. Although other mechanisms may underlie the antiviral activity, we hypothesize that one of the antiviral mechanisms of MCNA is NF-κB activation that is independent of IFN signaling.

Although several DAAs are currently in advanced clinical trials and the recently approved telaprevir and boceprevir combination therapies achieved high sustained virologic response rates, the frequent emergence of drug-resistant viruses is a major weakness of such agents. An ongoing search for more potent

and less toxic antiviral agents to improve anti-HCV chemotherapeutics is necessary. Our results indicate that MCNA and related *N*-(morpholine-4-carbonyloxy) amidine compounds constitute a new class of anti-HCV agents. Additional investigations elucidating their mechanism of action, and future modifications to improve anti-HCV activity, may open a new anti-HCV therapeutic window.

ACKNOWLEDGMENTS

We thank Frank Chisari for providing Huh7.5.1 cells, Takaji Wakita for providing the plasmid pJFH1full, and the Chemical Biology Screening Center of Tokyo Medical and Dental University for their assistance in this work.

This study was supported in part by grants from the Ministry of Education, Culture, Sports, Science and Technology of Japan; the Japan Society for the Promotion of Science, Ministry of Health, Labor and Welfare; the Japan Health Sciences Foundation; and the National Institute of Biomedical Innovation.

We declare that we have nothing to disclose regarding funding from industries or conflicts of interest with respect to the manuscript.

REFERENCES

1. Almstead NG, et al. 1999. Design, synthesis, and biological evaluation of potent thiazine- and thiazepine-based matrix metalloproteinase inhibitors. J. Med. Chem. 42:4547–4562.
2. Bailey M, Williams NA, Wilson AD, Stokes CR. 1992. PROBIT: weighted probit regression analysis for estimation of biological activity. J. Immunol. Methods 153:261–262.
3. Bigger CB, et al. 2004. Intrahepatic gene expression during chronic hepatitis C virus infection in chimpanzees. J. Virol. 78:13779–13792.
4. Flagothier C, Piérard-Franchimont C, Piérard GE. 2005. New insights into the effect of amorolfine nail lacquer. Mycoses 48:91–94.
5. Hickson I, et al. 2004. Identification and characterization of a novel and specific inhibitor of the ataxia-telangiectasia mutated kinase ATM. Cancer Res. 64:9152–9159.
6. Hoofnagle JH, Seeff LB. 2006. Peginterferon and ribavirin for chronic hepatitis C. N. Engl. J. Med. 355:2444–2451.
7. Horsmans Y, et al. 2005. Isatoribine, an agonist of TLR7, reduces plasma virus concentration in chronic hepatitis C infection. Hepatology 42:724–731.
8. Kanazawa N, et al. 2004. Regulation of hepatitis C virus replication by interferon regulatory factor 1. J. Virol. 78:9713–9720.
9. Karin M, Lin A. 2002. NF-kappaB at the crossroads of life and death. Nat. Immunol. 3:221–227.
10. Kim SS, et al. 2007. A cell-based, high-throughput screen for small molecule regulators of hepatitis C virus replication. Gastroenterology 132: 311–320.
11. Kwo PY, et al. 2010. Efficacy of boceprevir, an NS3 protease inhibitor, in combination with peginterferon alfa-2b and ribavirin in treatment-naive patients with genotype 1 hepatitis C infection (SPRINT-1): an open-label, randomised, multicentre phase 2 trial. Lancet 376:705–716.
12. Kwong AD, Kauffman RS, Hurter P, Mueller P. 2011. Discovery and development of telaprevir: an NS3-4A protease inhibitor for treating genotype 1 chronic hepatitis C virus. Nat. Biotechnol. 29:993–1003.
13. Lauer GM, Walker BD. 2001. Hepatitis C virus infection. N. Engl. J. Med. 345:41–52.
14. Levin JI, et al. 2005. Acetylenic TACE inhibitors. Part 2: SAR of six-membered cyclic sulfonamide hydroxamates. Bioorg. Med. Chem. Lett. 15:4345–4349.
15. Lipinski CA, Lombardo F, Dominy BW, Feeney PJ. 2001. Experimental and computational approaches to estimate solubility and permeability in drug discovery and development settings. Adv. Drug Deliv. Rev. 46:3–26.
16. Menear KA, et al. 2009. Identification and optimisation of novel and selective small molecular weight kinase inhibitors of mTOR. Bioorg. Med. Chem. Lett. 19:5898–5901.
17. Mishima K, et al. 2010. Cell culture and in vivo analyses of cytopathic hepatitis C virus mutants. Virology 405:361–369.
18. Nakagawa M, et al. 2004. Specific inhibition of hepatitis C virus replication by cyclosporin A. Biochem. Biophys. Res. Commun. 313:42–47.
19. Nakagawa M, et al. 2005. Suppression of hepatitis C virus replication by cyclosporin A is mediated by blockade of cyclophilins. Gastroenterology 129:1031–1041.
20. Peng LF, et al. 2007. Identification of novel epoxide inhibitors of hepatitis C virus replication using a high-throughput screen. Antimicrob. Agents Chemother. 51:3756–3759.
21. Polak A, Jäckel A, Noack A, Kappe R. 2004. Agar sublimation test for the in vitro determination of the antifungal activity of morpholine derivatives. Mycoses 47:184–192.
22. Poordad F, et al. 2011. Boceprevir for untreated chronic HCV genotype 1 infection. N. Engl. J. Med. 364:1195–1206.
23. Randall RE, Goodbourn S. 2008. Interferons and viruses: an interplay between induction, signalling, antiviral responses and virus countermeasures. J. Gen. Virol. 89:1–47.
24. Sakamoto N, et al. 2007. Bone morphogenetic protein-7 and interferon-alpha synergistically suppress hepatitis C virus replicon. Biochem. Biophys. Res. Commun. 357:467–473.
25. Sarrazin C, Zeuzem S. 2010. Resistance to direct antiviral agents in patients with hepatitis C virus infection. Gastroenterology 138:447–462.
26. Soothill JS, Ward R, Girling AJ. 1992. The IC50: an exactly defined measure of antibiotic sensitivity. J. Antimicrob. Chemother. 29:137–139.
27. Tai AW, et al. 2009. A functional genomic screen identifies cellular cofactors of hepatitis C virus replication. Cell Host Microbe 5:298–307.
28. Tanabe Y, et al. 2004. Synergistic inhibition of intracellular hepatitis C virus replication by combination of ribavirin and interferon-alpha. J. Infect. Dis. 189:1129–1139.
29. Wakita T, et al. 2005. Production of infectious hepatitis C virus in tissue culture from a cloned viral genome. Nat. Med. 11:791–796.
30. Walker EH, et al. 2000. Structural determinants of phosphoinositide 3-kinase inhibition by wortmannin, LY294002, quercetin, myricetin, and staurosporine. Mol. Cell 6:909–919.
31. Yokota T, et al. 2003. Inhibition of intracellular hepatitis C virus replication by synthetic and vector-derived small interfering RNAs. EMBO Rep. 4:602–608.
32. Zhong J, et al. 2005. Robust hepatitis C virus infection in vitro. Proc. Natl. Acad. Sci. U. S. A. 102:9294–9299.

Association of Gene Expression Involving Innate Immunity and Genetic Variation in Interleukin 28B With Antiviral Response

Yasuhiro Asahina,[1] Kaoru Tsuchiya,[1] Masaru Muraoka,[1,2] Keisuke Tanaka,[1,2] Yuichiro Suzuki,[1,2] Nobuharu Tamaki,[1] Yoshihide Hoshioka,[1] Yutaka Yasui,[1] Tomoji Katoh,[1] Takanori Hosokawa,[1] Ken Ueda,[1] Hiroyuki Nakanishi,[1] Jun Itakura,[1] Yuka Takahashi,[1] Masayuki Kurosaki,[1] Nobuyuki Enomoto,[2] Sayuri Nitta,[3] Naoya Sakamoto,[3] and Namiki Izumi[1]

Innate immunity plays an important role in host antiviral response to hepatitis C viral (HCV) infection. Recently, single nucleotide polymorphisms (SNPs) of *IL28B* and host response to peginterferon a (PEG-IFNa) and ribavirin (RBV) were shown to be strongly associated. We aimed to determine the gene expression involving innate immunity in *IL28B* genotypes and elucidate its relation to response to antiviral treatment. We genotyped *IL28B* SNPs (rs8099917 and rs12979860) in 88 chronic hepatitis C patients treated with PEG-IFNa-2b/RBV and quantified expressions of viral sensors (*RIG-I, MDA5*, and *LGP2*), adaptor molecule (*IPS-1*), related ubiquitin E3-ligase (*RNF125*), modulators (*ISG15* and *USP18*), and *IL28* (*IFNk*). Both *IL28B* SNPs were 100% identical; 54 patients possessed rs8099917 TT/rs12979860 CC (*IL28B* major patients) and 34 possessed rs8099917 TG/rs12979860 CT (*IL28B* minor patients). Hepatic expressions of viral sensors and modulators in *IL28B* minor patients were significantly up-regulated compared with that in *IL28B* major patients (≈3.3-fold, $P < 0.001$). However, expression of *IPS-1* was significantly lower in *IL28B* minor patients (1.2-fold, $P = 0.028$). Expressions of viral sensors and modulators were significantly higher in nonvirological responders (NVR) than that in others despite stratification by *IL28B* genotype (≈2.6-fold, $P < 0.001$). Multivariate and ROC analyses indicated that higher *RIG-I* and *ISG15* expressions and *RIG-I/IPS-1* expression ratio were independent factors for NVR. IPS-1 down-regulation in *IL28B* minor patients was confirmed by western blotting, and the extent of IPS-1 protein cleavage was associated with the variable treatment response. *Conclusion:* Gene expression involving innate immunity is strongly associated with *IL28B* genotype and response to PEG-IFNa/RBV. Both *IL28B* minor allele and higher *RIG-I* and *ISG15* expressions and *RIG-I/IPS-1* ratio are independent factors for NVR. (HEPATOLOGY 2012;55:20-29)

Infection with hepatitis C virus (HCV) is a common cause of chronic hepatitis, which progresses to liver cirrhosis and hepatocellular carcinoma in many patients.[1] Pegylated interferon α (PEG-IFNα) and ribavirin (RBV) combination therapy has been used to treat chronic hepatitis C (CH-C) to alter the natural course of this disease. However, 20% patients are nonvirological responders (NVR) whose HCV-RNA does not become negative during the 48 weeks of PEG-IFNα/RBV combination therapy.[2] In a recent genome-wide association study, single nucleotide polymorphisms (SNPs) located near interleukin 28B

Abbreviations: CH-C, chronic hepatitis C; γ-GTP, γ-glutamyl transpeptidase; GAPDH, glyceraldehyde-3-phosphate dehydrogenase; HCV, hepatitis C virus; HMBS, hydroxymethylbilane synthase; IL28, interleukin 28; IPS-1, IFNβ promoter stimulator 1; ISG15, interferon-stimulated gene 15; MDA5, melanoma differentiation associated gene 5; NVR; nonvirological responders; PEG-IFNα, pegylated interferonα; SNP, single nucleotide polymorphism; RIG-I, retinoic acid-inducible gene I; RBV, ribavirin; RNF125, ring-finger protein 125; ROC, receiver operator characteristic; SVR, sustained viral responder; TVR, transient virological responder; USP18, ubiquitin-specific protease 18; VR, virological responder.

From the [1]Department of Gastroenterology and Hepatology, Musashino Red Cross Hospital, Tokyo, Japan; [2]First Department of Internal Medicine, Faculty of Medicine, University of Yamanashi, Yamanashi, Japan; [3]Department of Gastroenterology and Hepatology, Tokyo Medical and Dental University, Tokyo, Japan.

Received May 14, 2011; accepted August 16, 2011.

Supported by grants from the Japanese Ministry of Education, Culture, Sports, Science and Technology and the Japanese Ministry of Welfare, Health and Labor. The funding source had no role in the collection, analysis, or interpretation of the data, or in the decision to submit the article for publication.

(*IL28B*) that encodes for type III IFNλ3 were shown to be strongly associated with a virological response to PEG-IFNα/RBV combination therapy.[3-5] In particular, the rs8099917 TG and GG genotypes were shown to be strongly associated with a null virological response to PEG-IFNα/RBV.[3] However, mechanisms involving resistance to PEG-IFNα/RBV have not been completely elucidated.

The innate immune system has an essential role in host antiviral defense against HCV infection.[6] The retinoic acid-inducible gene I (RIG-I), a cytoplasmic RNA helicase, and related melanoma differentiation associated gene 5 (MDA5) play essential roles in initiating the host antiviral response by detecting intracellular viral RNA.[7,8] The IFNβ promoter stimulator 1 (IPS-1)—also called the caspase-recruiting domain adaptor inducing IFNβ, mitochondrial antiviral signaling protein, or virus-induced signaling adaptor—is an adaptor molecule. IPS-1 connects RIG-I sensing to downstream signaling, resulting in *IFNβ* gene activation.[9-12] RIG-I sensing of incoming viral RNA has been shown to be modified by LGP2,[8,13] a helicase related to RIG-I and MDA5 lacking caspase-recruiting domain. The ubiquitin ligase ring-finger protein 125 (RNF125) has been shown to conjugate ubiquitin to RIG-I, MDA5, and IPS-1 and this suppresses the functions of these proteins.[14] Further, these molecules are ISGylated by the IFN-stimulated gene 15 (ISG15), a ubiquitin-like protein,[15] and ISG15 is specifically removed from ISGylated protein by ubiquitin-specific protease 18 (USP18) to regulate the RIG-I/IPS-1 system.[16,17] Moreover, the NS3/4A protease of HCV specifically cleaves IPS-1 as part of its immune-evasion strategy.[9,18] Therefore, the RIG-I/IPS-1 system and its regulatory systems have essential roles in the innate antiviral response.

Recently, we demonstrated that baseline intrahepatic gene expression levels of the RIG-I/IPS-1 system were prognostic biomarkers of the final virological outcome in CH-C patients who were treated with PEG-IFNα/RBV combination therapy.[19] We found that up-regulation of *RIG-I* and *ISG15* and a higher expression ratio of *RIG-I/IPS-1* could predict NVR for subsequent treatment with PEG-IFNα/RBV combination therapy.[19] However, association of gene expression involving innate immunity and genetic variation of *IL28B* has not yet been elucidated. Hence, the aim of this study was to determine gene expression involving the innate immune system in different genetic variations of *IL28B* and elucidate the relation of gene expression to final virological outcome of PEG-IFNα/RBV combination therapy in CH-C patients.

Patients and Methods

Patients. Among histologically proven CH-C patients admitted at the Musashino Red Cross Hospital, 88 patients with HCV genotype 1b and a high viral load (>5 log IU/mL by TaqMan HCV assay; Roche Molecular Diagnostics, Tokyo, Japan) were included in the present study (Table 1). Patients with decompensated liver cirrhosis, autoimmune hepatitis, or alcoholic liver injury were excluded. No patient had tested positive for hepatitis B surface antigen or anti-human immunodeficiency virus antibody or had received immunomodulatory therapy before enrollment. Forty-two patients had been enrolled in a previous study that determined hepatic gene expression involving innate immunity.[19] Written informed consent was obtained from all patients and the study was approved by the Ethical Committee of Musashino Red Cross Hospital in accordance with the Declaration of Helsinki.

Treatment Protocol. The patients were administered subcutaneous injections of PEG-IFNα-2b (PegIntron, MSD, Whitehouse Station, NJ) at a dose of 1.5 μg kg^{-1} week^{-1} for 48 weeks. RBV (Rebetol, MSD) was administered concomitantly over this treatment period, administered orally twice daily at 600 mg/day for patients who weighed less than 60 kg and 800 mg/day for patients who weighed between 60-80 kg. The dose of PEG-IFNα-2b was reduced to 0.75 μg kg^{-1} week^{-1} when either neutrophil count was less than 750/mm^3 or platelet count was less than 80 $\times$ 10^3/mm^3. The dose of RBV was reduced to 600 mg/day when the hemoglobin concentration decreased to 10 g/dL. More than 80% adherence was achieved in all patients.

Measurement of Hepatic Gene Expression. Liver biopsy was performed immediately before initiating

Address reprint requests to: Namiki Izumi, M.D., Ph.D., Chief, Department of Gastroenterology and Hepatology, Musashino Red Cross Hospital, 1-26-1 Kyonancho 1-26-1, Musashinoshi, Tokyo 180-8610, Japan. E-mail: nizumi@musashino.jrc.or.jp; fax: +81-422-32-9551.

View this article online at wileyonlinelibrary.com.

DOI 10.1002/hep.24623

Potential conflict of interest: Nothing to report.

Additional Supporting Information may be found in the online version of this article.

Table 1. Patient Characteristics and *IL28B* Genotype

	IL28B Major*	*IL28B* Minor†	*P*-value‡
Patients, n	54	34	
Age (SD), year	58.8 (10.0)	59.1 (10.3)	0.918§
Sex, n (%)			0.051‖
Male	13 (24.1)	15 (44.1)	
Female	41 (75.9)	19 (55.9)	
BMI (SD), kg/m^2	22.7 (3.5)	23.5 (3.6)	0.193§
ALT (SD), IU/L	61.3 (50.7)	62.4 (44.7)	0.962§
γ-GTP (SD), IU/L	36.7 (25.9)	57.3 (52.4)	0.010§
LDL-cholesterol (SD), mg/dL	103.3 (29.8)	91.8 (26.9)	0.067§
Hemoglobin (SD), g/dL	14.1 (1.4)	14.4 (1.3)	0.186§
Platelet count (SD), ×10^{3}3/μL	161 (6.4)	163 (4.4)	0.489§
Fibrosis stage, n (%)			0.532‖
F1, 2	38 (70.4)	26 (76.5)	
F3, 4	16 (29.6)	8 (23.5)	
Viral load (SD), ×10^{63} IU/mL	1.7 (1.4)	1.9 (2.0)	0.788§
%HCV core 70 & 91 a.a. double mutation¶	8.9	43.5	0.001‖
%ISDR wild**	43.5	51.7	0.486‖
Viral response, n (%)			<0.001‖
SVR	17 (31.5)	13 (38.2)	
TVR	26 (48.1)	3 (8.8)	
NVR	11 (20.4)	18 (52.9)	

Unless otherwise indicated, data are given as mean (SD).

*rs8099917 TT and rs12979860 CC.

†rs8099917 TG and rs12979860 CT.

BMI, body mass index; ALT, alanine aminotransferase; γ-GTP, γ-glutamyl transpeptidase; LDL-C, low-density lipoprotein cholesterol; HCV, hepatitis C virus; ISDR, interferon sensitivity determining region; SVR, sustained virological response; TVR, transient virological response; NVR, nonvirological response.

‡Comparison between *IL28B* major and minor genotypes.

§Mann-Whitney *U* test.

‖Chi-square test.

¶HCV core mutation was determined in 68 patients.

**ISDR was determined in 75 patients.

the therapy. After extraction of total RNA from liver biopsy specimens, the messenger RNA (mRNA) expression of the positive and negative cytoplasmic viral sensor (*RIG-I, MDA5*, and *LGP2*), the adaptor molecule (*IPS-1*), the related ubiquitin E3-ligase (*RNF125*), the modulators of these molecules (*ISG15* and *USP18*), and *IFNλ* (*IL28A/B*) was quantified by real-time quantitative polymerase chain reaction (PCR) using target gene-specific primers. In brief, total RNA was extracted by the acid-guanidinium-phenol-chloroform method using Isogen reagent (Nippon Gene, Toyama, Japan) from the liver biopsy specimen, which was 0.2-0.4 cm in length and 13G in diameter. Complementary DNA (cDNA) was transcribed from 2 μg of total RNA template in a 140-μL reaction mixture using the SYBR RT-PCR Kit (Takara Bio, Otsu, Japan) with random hexamer. Real-time quantitative PCR was performed using Smart Cycler version II (Takara Bio) with the SYBR RT-PCR Kit (Takara Bio) according to the manufacturer's instructions. Assays were performed in duplicate and the expression levels of target genes were normalized to the expressions of glyceraldehyde-3-phosphate dehydrogenase (*GAPDH*) gene and hydroxymethylbilane synthase (*HMBS*), an enzyme that is stable in the liver, as quantified using real-time quantitative PCR as internal controls. For accurate normalization, a set of two housekeeping genes was used in the present study. Sequences of the primer sets were as follows: *RIG-I*, 5′-AAAGCATGCA TGGTGTTCCAGA-3′, 5′-TCATTCGTGCATGCTC ACTGATAA-3′; *MDA5*, 5′-ACATAACAGCAACATG GGCAGTG-3′, 5′-TTTGGTAAGGCCTGAGCTGG AG-3′; *LGP2*, 5′-ACAGCCTTGCAAACAGTACAAC CTC-3′, 5′-GTCCCAAATTTCCGGCTCAAC-3′; *IPS-1*, 5′-GGTGCCATCCAAAGTGCCTACTA-3′, 5′-CAGC ACGCCAGGCTTACTCA-3′; *RNF125*, 5′-AGGGCA CATATTCGGACTTGTCA-3′, 5′-CGGGTATTAAAC GGCAAAGTGG-3′; *ISG15*, 5′-AGCGAACTCATCT TTGCCAGTACA-3′, 5′-CAGCTCTGACACCGACA TGGA-3′; *USP18*, 5′-TGGTTCTGCTTCAATGACT CCAATA-3′, 5′-TTTGGGCATTTCCATTAGCACT C-3′; *IFNλ*: 5′-CAGCTGCAGGTGAGGGA-3′, 5′-G GTGGCCTCCAGAACCTT-3′; *GAPDH*, 5′-GCACC GTCAAGGCTGAGAAC-3′, 5′-ATGGTGGTGAAGA CGCCAGT-3′; *HMBS*, 5′-AAGCGGAGCCATGTCT GGTAAC-3′, 5′-GTACCCACGCGAATCACTCTCA-3′.

Genotyping for* IL28B *(rs8099917 and rs12979860) Polymorphism. Genetic polymorphism in a tagged SNP located near the *IL28B* gene (rs8099917 and rs12979860) was determined by direct sequencing of PCR-amplified DNA. In brief, after extraction from whole blood samples, genomic DNA was amplified by PCR. Sequences of the primer sets were: rs8099917, 5′-ATCCTCCTCTCATCCCTCA TC-3′, 5′-GGTATCAACCCCACCTCAAAT-3′; rs129 79860, 5′-GGACGAGAGGGCGTTAGAG-3′, 5′-AG GGACCGCTACGTAAGTCAC-3′.

Both strands of the PCR products were sequenced by the dye terminator method using BigDye Terminator v3.1 Cycle Sequencing Kit (Applied Biosystems, Chiba, Japan); nucleotide sequences were determined by a capillary DNA sequencer ABI3730xl (Applied Biosystems). Homozygosity (rs8099917 GG and rs12979860 TT) or heterozygosity (rs8099917 TG and rs12979860 CT) of the minor sequence was defined as having the *IL28B* minor allele, whereas homozygosity for the major sequence (rs8099917 TT and rs12979860 CC) was defined as having the *IL28B* major allele.

Western Blotting. Western blotting was performed using samples from 14 patients (six from *IL28B* major patients and eight from *IL28B* minor patients) as described.[19] In brief, liver biopsy specimens of

approximately 10 mg were homogenized in 100 μL of Complete Lysis-M (Roche Applied Science, Penzberg, Germany). Next, 30 μg of protein was separated by NuPAGE 4%-12% Bis-Tris gels (Invitrogen, Carlsbad, CA) and blotted on polyvinylidene difluoride membranes. The membranes were immunoblotted with anti-RIG-I (Cell Signaling Technology, Danvers, MA) or anti-IPS-1 (Enzo Life Science, Farmingdale, NY), followed by anti-β-actin (Sigma Aldrich, St. Louis, MO). After immunoblotting with horseradish peroxidase-conjugated secondary antibody, signals were detected by chemiluminescence (BM Chemiluminescence Blotting Substrate, Roche Applied Science, Mannheim, Germany). Optical densitometry was performed using ImageJ software (NIH, Bethesda, MD). Naive Huh7 cells were used for a positive control for full-length IPS-1, and cells transfected with HCV-1b subgenomic replicon[20] were used for a positive control for cleaved IPS-1.

Definitions of Response to Therapy. A patient negative for serum HCV-RNA during the first 6 months after completing PEG-IFNα-2b/RBV combination therapy was defined as a sustained viral responder (SVR), and a patient for whom HCV-RNA became negative at the end of therapy and reappeared after completion of therapy was defined as a transient virological responder (TVR). A patient for whom HCV-RNA became negative at the end of therapy (SVR + TVR) was defined as a virological responder (VR). A patient whose HCV-RNA did not become negative during the course of therapy was defined as an NVR. HCV-RNA was determined by TaqMan HCV assay (Roche Molecular Diagnostics).

Statistical Analysis. Categorical data were compared using the chi-square test and Fisher's exact test. Distributions of continuous variables were analyzed by the Mann-Whitney *U* test for two groups. All tests of significance were two-tailed and $P < 0.05$ was considered statistically significant.

Results

Patient Characteristics and* IL28B *Genotype. Table 1 shows patient characteristics according to *IL28B* genotype. SNPs at rs8099917 and rs12979860 were 100% identical; 54 patients were identified as having the major alleles (rs8099917 TT/rs12979860 CC; *IL28B* major patients) and the remaining 34 had the minor alleles (rs8099917 TG/rs12979860 CT; *IL28B* minor patients). Patients having a minor homozygote (rs8099917 GG or rs12979860 TT) were not found in this study, which is consistent with a recent report of the rarity of a minor homozygote in Japanese patients.[3] *IL28B* minor patients were significantly associated with a higher γ-glutamyl transpeptidase (γ-GTP) level and higher frequency of mutations at amino acid positions 70 and 91 of the HCV core region (glutamine or histidine mutation at amino acid position 70; methionine mutation at amino acid position 91). NVR rate was significantly higher in *IL28B* minor patients than in *IL28B* major patients.

Gene Expression Involving Innate Immunity and* IFNλ *in the Liver. Hepatic expression levels of cytoplasmic viral sensors (*RIG-I, MDA5*, and *LGP2*) were significantly higher in *IL28B* minor patients than in *IL28B* major patients (Fig. 1). Similarly, expressions of *ISG15* and *USP18* were significantly higher in *IL28B* minor patients than in *IL28B* major patients (Fig. 1). In contrast, the hepatic expression of the adaptor molecule (*IPS-1*) was significantly lower in *IL28B* minor patients than that in *IL28B* major patients (Fig. 1). Hepatic expression of *RNF125* was similar among *IL28B* genotypes (Fig. 1). *IFNλ (IL28A/B)* expression was higher in *IL28B* minor patients, but not statistically significant (Fig. 1). Because expression of *RIG-I* and *IPS-1* were negatively correlated, the expression ratio of *RIG-I/IPS-1* in *IL28B* minor patients was significantly higher than in *IL28B* major patients (Fig. 1).

Next, to assess the relationship between baseline hepatic gene expression and treatment efficacy, we compared levels of gene expression involving innate immunity and *IFNλ* based on the final virological response (Fig. 2). Overall, hepatic expressions of cytoplasmic viral sensors and the ISG15/USP18 system in NVR patients were significantly higher than those in VR patients. In a similar but opposite manner, hepatic expressions of *IPS-1* and *RNF125* in NVR patients were significantly lower than that in VR patients, and the expression of *IFNδ* was higher in NVR patients, but the differences were not statistically significant. Expression ratio of *RIG-I/IPS-1* was significantly higher in NVR patients than that in VR patients.

Because hepatic expressions of the RIG-I/IPS-1 and ISG15/USP18 systems were significantly related both to *IL28B* minor and NVR patients, *RIG-I* and *ISG15* expression levels and the *RIG-I/IPS-1* ratio between VR and NVR patients were further stratified by *IL28B* genotype (Fig. 3). Even in the subgroup of *IL28B* minor patients, the expressions of *RIG-I* and *ISG15* were significantly higher in NVR patients than those in VR patients. Similar tendencies were observed in a subgroup of *IL28B* major patients, in whom the *RIG-I/IPS-1* expression ratio was significantly higher in

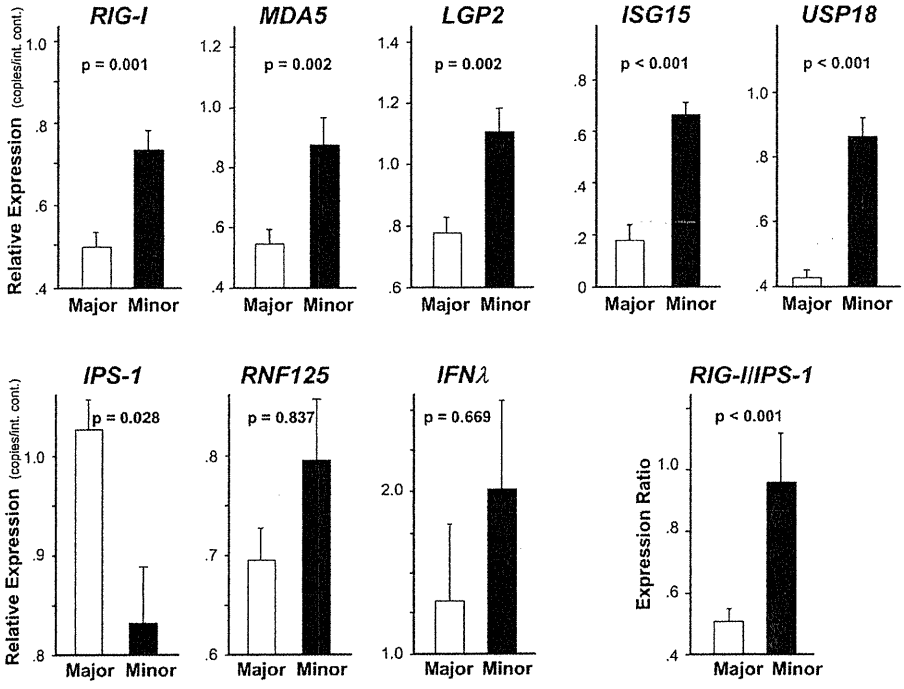

Fig. 1. Comparison of hepatic gene expression levels between *IL28B* major (rs8099917 TT/rs12979860 CC, n = 54) and *IL28B* minor patients (rs8099917 TG/rs12979860 CT, n = 34). Expression levels of cytoplasmic viral sensors (*RIG-I*, *MDA5*, and *LGP2*), modulators (*ISG15* and *USP18*), an adaptor (*IPS-1*), negative regulators (*RNF125*) and *IFNλ*, and expression ratio of the *RIG-I/IPS-1* are shown. Error bars indicate standard error. The *P*-values were determined by the Mann-Whitney *U* test.

NVR patients than in VR patients. However, in patients of the same virological response subgroup, *RIG-I* and *ISG15* expression levels and *RIG-I/IPS-1* ratio were higher in *IL28B* minor patients, and the difference in *ISG15* expression in subgroup of VR and NVR patients and that in *RIG-I/IPS-1* ratio in subgroup of VR patients was statistically significant between *IL28B* genotypes (Fig. 3).

Receiver Operator Characteristic (ROC) Analysis. To determine the usefulness of these gene quantifications and *IL28B* genotyping as predictors of NVR, an ROC analysis was conducted (Fig. 4A). The area under the ROC curve for *RIG-I* and *ISG15* expressions and *RIG-I/IPS-1* expression ratio was 0.712, 0.782, and 0.732, respectively, suggesting that quantification of these gene transcripts is useful for

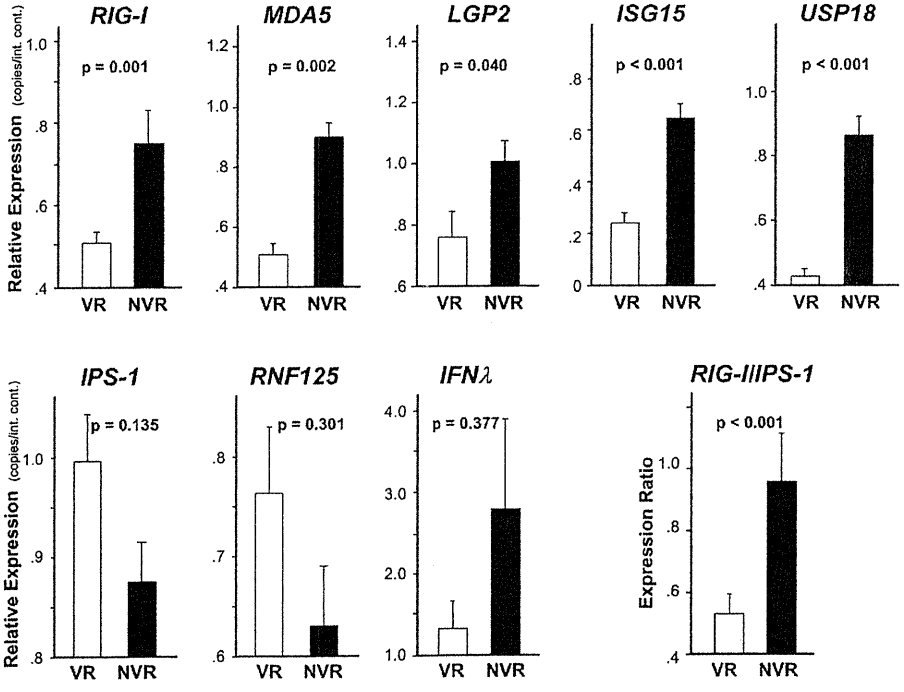

Fig. 2. Comparison of hepatic gene expression levels between virological responders (VR, n = 60) and nonvirological responders (NVR, n = 28). Expression levels of cytoplasmic viral sensors (*RIG-I*, *MDA5*, and *LGP2*), modulators (*ISG15* and *USP18*), an adaptor (*IPS-1*), negative regulators (*RNF125*) and *IFNλ*, and *RIG-I/IPS-1* expression ratio are shown. Error bars indicate standard error. The *P*-values were determined by the Mann-Whitney *U* test.

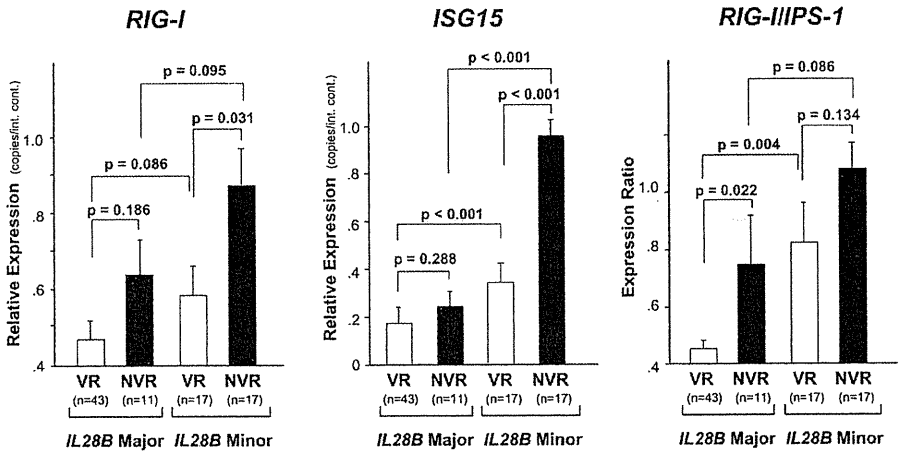

Fig. 3. Comparison of hepatic gene expression levels between virological responders (VR) and nonvirological responders (NVR) in subgroups of the *IL28B* genotype (*IL28B* Major, rs8099917 TT/rs12979860 CC; *IL28B* Minor, rs8099917 TG/rs12979860 CT). Expressions of *RIG-I* and *ISG15* as well as the *RIG-I/IPS-1* expression ratio are shown. Error bars indicate standard error. The numbers of patients in each subgroup are shown in the bottom of the figure.

prediction of NVR (Table 2). The area under the ROC curve for *IL28B* genotype was 0.662, which was lower compared with that for *RIG-I* and *ISG15* expressions and *RIG-I/IPS-1* ratio.

When we stratified the patients by the cutoff value for *RIG-I* and *ISG15* expressions and *RIGI/IPS-1* ratio, no statistically significant difference was found in NVR rates among *IL28B* genotypes within the same subgroup (Fig. 4B).

Factors Associated with NVR. In univariate analysis, age, platelet counts, double mutation at amino acid positions 70 and 91 of the HCV core region, *IL28B* minor allele, and hepatic expressions of *RIG-I, MDA5, LGP2, ISG15,* and *USP18,* and *RIG-I/IPS-1* ratio were significantly

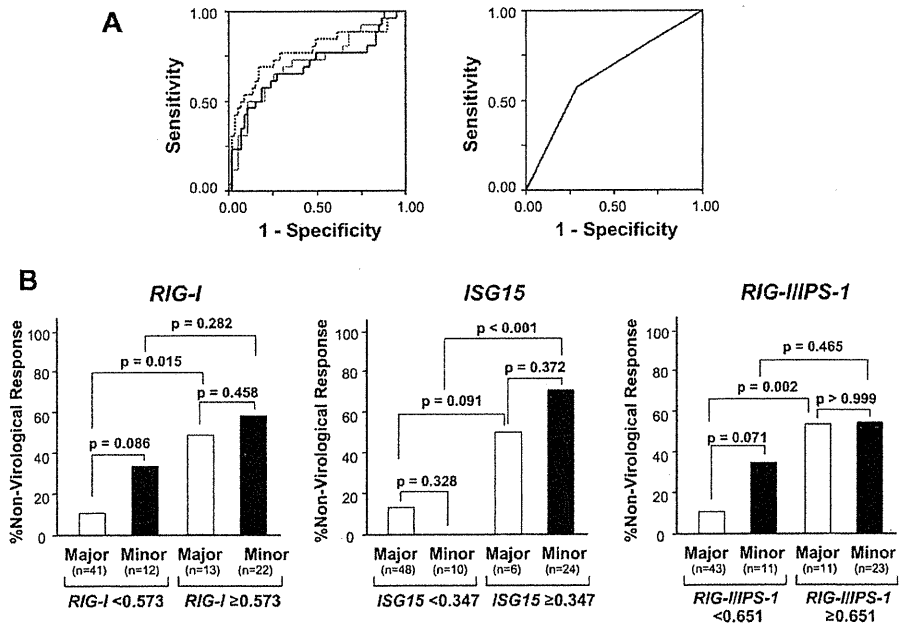

Fig. 4. (A) Receiver operator characteristics (ROC) curve for prediction of nonvirological response. ROC curves were generated to compare *RIG-I* (black line), *ISG15* (dotted line), and *RIG-I/IPS-1* ratio (gray line) (all in the left panel), and *IL28B* genotype (in the right panel). (B) Nonvirological response rate in *IL28B* major (rs8099917 TT/rs12979860 CC) and minor patients (rs8099917 TG/rs12979860 CT) in subgroups divided by the cutoff value of *RIG-I* and *ISG15* expression and the *RIG-I/ISG15* ratio determined by ROC analysis. Cutoff values of *RIG-I* and *ISG15* expression are expressed as expression copy number normalized to the expression of an internal control. The numbers of patients in each subgroup are shown in the bottom of the figure.

Table 2. Area Under the ROC Curves, Sensitivity, Specificity, and Negative as Well as Positive Predictive Values of Nonvirological Responses

Variables	AUC	95% CI	Cutoff	Sensitivity	Specificity	NPV	PPV
RIG-I (copies/int. control)	0.712	0.584-0.840	0.573	0.679	0.733	0.830	0.543
ISG15 (copies/int. control)	0.782	0.666-0.899	0.347	0.714	0.833	0.862	0.667
RIG-I/IPS-1 (copies/int. control)	0.732	0.611-0.852	0.651	0.679	0.750	0.833	0.559
IL28B genotype	0.662	0.537-0.787	TG*/CT†	0.607	0.717	0.796	0.500

AUC, area under the curve; NPV, negative predictive value; PPV, positive predictive value.
*Genotype at rs8099917.
†Genotype at rs12979860.

associated with NVR (Table 3). Among these, multivariate analysis identified old age, HCV core double mutant, and higher hepatic expressions of *RIG-I* and *ISG15* as factors independently associated with NVR (Table 3).

IPS-1 and RIG-I Protein Expression in the Liver. Western blotting revealed that full-length and cleaved IPS-1 were variably present in all the samples from CH-C patients (Fig. 5A). Similar to mRNA

Table 3. Factors Associated with Nonvirological Response

	Univariate Analysis		Multivariate Analysis*	
Factors	Risk Ratio (95% CI)	*P*-value	Risk Ratio (95% CI)	*P*-value
Age (by every 10 year)	1.84 (1.10-3.14)	0.027	3.76 (1.19-11.7)	0.023
Sex				
Male	1			
Female	1.62 (0.59-4.42)	0.350		
BMI (by every 5 kg/m^2)	0.87 (0.46-1.65)	0.672		
Fibrosis stage				
F1/F2	1			
F3/F4	1.82 (0.69-4.85)	0.228		
Degree of steatosis				
<10%	1			
≥10%	1.46 (0.43-5.03)	0.544		
Albumin (by every 1 g/dL)	0.41 (0.11-1.56)	0.190		
AST (by every 40 IU/L)	0.89 (0.53-1.56)	0.681		
ALT (by every 40 IU/L)	0.85 (0.57-1.32)	0.481		
γ-GTP (by every 40 IU/L)	1.32 (0.82-2.07)	0.235		
Fasting blood sugar (by every 100 mg/dL)	1.35 (0.74-2.45)	0.340		
Hemoglobin (by every 1 g/dL)	0.93 (0.67-1.31)	0.683		
Platelet counts (by every 10^4/μL)	0.90 (0.82-0.99)	0.037	0.92 (0.78-1.08)	0.296
HCV load (by every 100 KIU/mL)	1.00 (1.00-1.00)	0.688		
Core 70 & 91 double mutation				
Wild	1		1	
Mutant	3.92 (1.14-13.5)	0.030	11.1 (1.40-88.7)	0.023
ISDR				
Nonwildtype	1			
Wildtype	1.38 (0.13-3.61)	0.513		
IL28B genotype				
Major allele†	1		1	
Minor allele‡	3.91 (1.52-10.0)	0.005	1.53 (0.20-11.9)	0.684
Hepatic gene expression (by every 0.1 copy/*int. control*)				
RIG-I	1.28 (1.10-1.50)	0.002	1.53 (1.07-2.22)	0.021
MDA5	1.53 (1.12-2.00)	0.001		
LGP2	1.34 (1.04-1.74)	0.026		
IPS-1	0.90 (0.78-1.04)	0.143		
RNF125	0.93 (0.83-1.04)	0.204		
ISG15	1.37 (1.16-1.62)	<0.001	1.28 (1.04-1.58)	0.021
USP18	1.67 (1.27-2.20)	<0.001		
IFNλ	1.02 (0.99-1.05)	0.170		
RIG-I/IPS-1 ratio (by every 0.1)	1.21 (1.07-1.36)	0.002		

Risk ratios for nonvirological response were calculated by the logistic regression analysis. BMI, body mass index; AST, aspartate aminotransferase; ALT, alanine aminotransferase; γ-GTP, gamma-glutamyl transpeptidase; HCV, hepatitis C virus; ISDR, IFN sensitivity determining region.
*Multivariate analysis was performed with factors significantly associated with nonvirological response by univariate analysis except for *MDA5*, *LGP2*, *USP18*, and *RIG-I/IPS-1* ratio, which were significantly correlated with *RIG-I* and *ISG15*.
†rs8099917 TT and rs12979860 CC.
‡rs8099917 TG and rs12979860 CT.

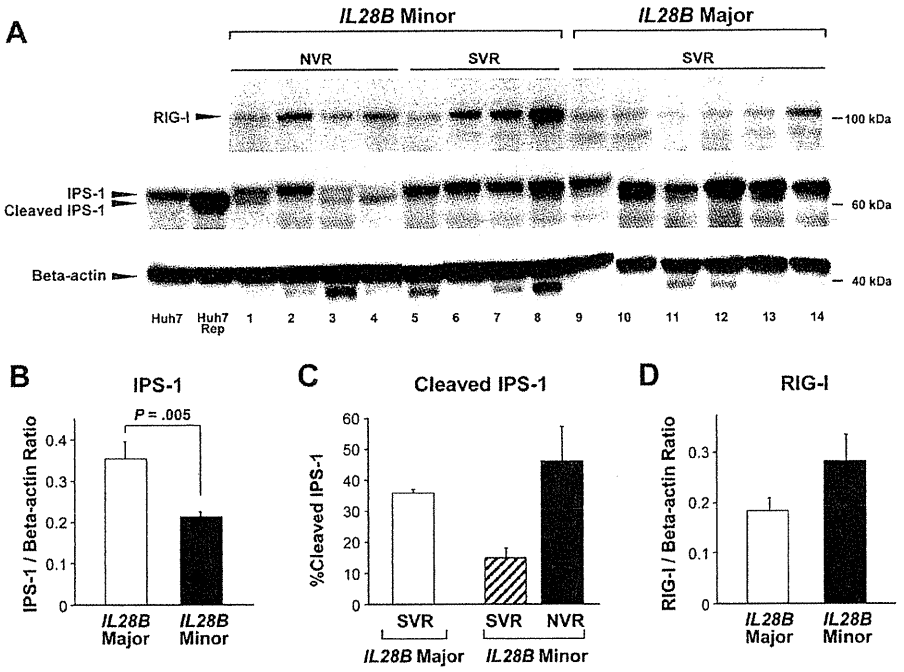

Fig. 5. (A) Western blotting for IPS-1 and RIG-I protein expression levels. Eight lanes contain samples from *IL28B* minor patients (lanes 1-8) and six lanes contain samples from *IL28B* major patients (lanes 9-14). Four lanes contain samples from nonvirological responders (NVR, lanes 1-4) and 10 lanes contain samples from sustained virological responders (SVR, lanes 5-14). Specific bands for RIG-I, full-length IPS-1, cleaved IPS-1, and β-actin are indicated by arrows. Naive Huh7 cells were used for a positive control for full-length IPS-1 (lane Huh7), and cells transfected with HCV-1b subgenomic replicon (Reference #20) were used for a positive control for cleaved IPS-1 (lane Huh7 Rep). (B) Total IPS-1 protein expression levels normalized to β-actin according to *IL28B* genotype. Error bars indicate standard error. *P*-value was determined by Mann-Whitney *U* test. (C) Percentage of cleaved IPS-1 products in total IPS-1 protein according to treatment responses stratified by *IL28B* genotype. Error bars indicate standard error. (D) RIG-I protein expression levels normalized to β-actin according to *IL28B* genotype. Error bars indicate standard error.

expression, total hepatic IPS-1 protein expression was significantly lower in *IL28B* minor patients than in *IL28B* major patients (Fig. 5B). With regard to *IL28B* minor patients, the percentage of cleaved IPS-1 protein in total IPS-1 in SVR was lower than that in NVR (Fig. 5C). In contrast to IPS-1 protein expression, hepatic RIG-I protein expression was higher in *IL28B* minor patients than that in *IL28B* major patients (Fig. 5D).

Discussion

In the present study we found that the baseline expression levels of intrahepatic viral sensors and related regulatory molecules were significantly associated with the genetic variation of *IL28B* and final virological outcome in CH-C patients treated with PEG-IFNα/RBV combination therapy. Although the relationship between the *IL28B* minor allele and NVR in PEG-IFNα/RBV combination therapy is evident, mechanisms responsible for this association remain unknown. *In vitro* studies have suggested that cytoplasmic viral sensors, such as RIG-I and MDA5, play a pivotal role in the regulation of IFN production and augment IFN production through an amplification circuit.[7,8] Our results indicate that expressions of *RIG-I* and *MDA5* and a related amplification system may be up-regulated by endogenous IFN at a higher baseline level in *IL28B* minor patients. However, HCV elimination by subsequent exogenous IFN is insufficient in these patients, as reported,[19] suggesting that *IL28B* minor patients may have adopted a different equilibrium in their innate immune response to HCV. Our data are further supported by recent reports of an association between intrahepatic levels of IFN-stimulated gene expression and PEG-IFNα/RBV response as well as with *IL28B* genotype.[21-23]

In contrast to cytoplasmic viral sensor (*RIG-I, MDA5*, and *LGP2*) and modulator (*ISG15* and *USP18*) expression, the adaptor molecule (*IPS-1*) expression was significantly lower in *IL28B* minor patients. Moreover, western blotting further confirmed IPS-1 protein downregulation in *IL28B* minor patients by revealing decreased protein levels. Because IPS-1 is one of the main target molecules of HCV evasion,[9,18]